Kinetic oscillations in the NO + CO reaction on Pt(100): Experiments and mathematical modeling

Cite as: J. Chem. Phys. **95**, 2109 (1991); https://doi.org/10.1063/1.461010
Submitted: 26 November 1990 • Accepted: 15 April 1991 • Published Online: 31 August 1998

Th. Fink, J.-P. Dath, R. Imbihl, et al.

Kinetic oscillations in the NO + CO reaction on Pt(100): Experiments and mathematical modeling

Th. Fink, J.-P. Dath,[a] R. Imbihl, and G. Ertl
Fritz Haber Institut der Max Planck Gesellschaft, Faradayweg 4-6, D 1000 Berlin 33, Germany

(Received 26 November 1990; accepted 15 April 1991)

The reaction of NO and CO on Pt(100) exhibits two branches of steady state production of N_2 and CO_2 and the occurrence of kinetic oscillations. This system was studied under steady flow conditions in the 10^{-6} mbar total pressure range using low-energy electron diffraction-(LEED), work function measurement, and mass spectrometry for determination of the reaction rate. These studies revealed that kinetic oscillations can only be initiated from one of the two stable reaction branches. Two separate existence regions were detected in which the oscillations are always damped. Oscillations can be very reproducibly excited by slight decreases in temperature. The $1\times1\rightleftharpoons$hex phase transition of the surface structure was observed to take place only in one of the two regions of reaction rate oscillations. Its influence seems to be of minor relevance to the mechanism of oscillations as oscillations in one region occur on the surface that maintains a 1×1 structure. The experiments were modeled by a set of coupled differential equations based on knowledge about the elementary reaction steps. The model calculations reproduced the steady states of the reaction as well as the occurrence of kinetic oscillations in different ranges in excellent agreement with experimental observation. In the model, the phase transition also has no relevance for the oscillation mechanism. The occurrence of oscillations can be rationalized in terms of a periodic sequence of autocatalytic "surface explosions" and the restoration of an adsorbate-covered surface. The damping, experimentally observed, is attributed to insufficient spatial coupling between different regions of the surface.

I. INTRODUCTION

Kinetic oscillations in the catalytic oxidation of CO, first discovered with polycrystalline Pt as the catalyst,[1,2] have been studied extensively in the past decade on various Pt single crystal surfaces in the low pressure range (10^{-6}–10^{-3} mbar).[3,4] Using surface sensitive techniques, the mechanism of kinetic oscillations was found to be coupled to periodic structural transformations of the surface, namely, the CO-induced $1\times1\rightleftharpoons1\times2$ and $1\times1\rightleftharpoons$hex phase transition on Pt(110) and Pt(100), respectively. Besides an experimental verification of the relevance of these phase changes to the mechanism, a variety of new and interesting phenomena were discovered in these studies. These included transitions to chaos, chemical waves, the formation of Turing structures and of complex spatiotemporal patterns.[3,4]

While quite a number of heterogeneously catalyzed reactions exhibit kinetic oscillations under appropriate conditions, the only reaction system which so far has been investigated in single crystal studies, apart from the $CO + O_2$ reaction, is the system Pt(100)/$NO + CO \rightarrow CO_2 + 1/2\ N_2$). Kinetic oscillations in this system were discovered by Singh-Boparai and King[5] at extremely low pressure in the 10^{-9} mbar range, and were later systematically studied by Schwartz and Schmidt[6,7] in the pressure range from 10^{-8} to 10^{-5} mbar. Kinetic oscillations in the NO + CO reaction were also found with polycrystalline Pt in the 10^{-4} mbar region by Lintz *et al.*[8,9] Using Fourier transform infrared (FTIR) spectroscopy and supported Pt and Pd as catalysts, these investigations were extended to atmospheric pressure conditions by Schüth and Wicke.[10]

Although some suggestions have been presented for the mechanism involved, in none of these studies were the experimental results conclusive enough to support a detailed mechanistic picture for kinetic oscillations. Since it has been shown that the $1\times1\rightleftharpoons$hex phase transition is the driving force for kinetic oscillations in the low pressure $CO + O_2$ reaction on Pt(100),[11,12] the primary aim of the present study has been to determine experimentally the role of the phase transition in the NO + CO reaction. The study of kinetic oscillations was complemented by an investigation of the so-called "surface explosion." In this process, coadsorbed NO and CO react to form extremely narrow temperature programmed reaction (TPR) peaks of N_2 and CO_2 [full width at half-maximum (FWHM) ~2–3 K].[13,14] However, the origin of the "explosive" product formation had not been clarified unambiguously.

It was found that the kinetic oscillations and the surface explosion occur in about the same temperature region and are closely related via the autocatalytic behavior of the surface reaction. The autocatalytic reaction mechanism of the NO + CO reaction is responsible for the sharpness of the TPR product peaks in the surface explosion and it is also the main driving force for kinetic oscillations under stationary conditions. These conclusions were confirmed by a mathematical model based on a set of coupled differential equations (DE's). With this model, both the surface explosion and the kinetic oscillations could be reproduced successfully

[a] Laboratoire de Chimie Inorganique et Analytique, Faculté des Sciences, Université de l'Etat à Mons, 23, Avenue Maistriau, B 7000 Mons, Belgium.

 0021-9606/91/152109-18$03.00

using experimentally determined values for the rate laws and reaction-process parameters. In this paper, the experimental results and the numerical simulation of kinetic oscillations are presented. Results concerning the surface explosion are published elsewhere.[15,16]

II. EXPERIMENTAL

Experiments were performed in a standard stainless steel ultra high-vacuum (UHV) system. A base pressure of 2×10^{-10} mbar was achieved by using a combination of a turbo-molecular pump (360 ℓ/s), an ion getter pump (180 ℓ/s), and a titanium sublimation pump. Sample surface characteristics were studied using a piezoelectric driven Kelvin probe[17] for work function measurement and a four-grid rear-view low-energy electron diffraction (LEED) optics (Omicron). Quantitative information about structural changes was obtained by monitoring LEED spot intensities in real time using a video-LEED system described elsewhere.[18] For residual gas analysis in temperature programmed desorption (TPD) experiments and in reaction rate measurements, two quadrupole mass spectrometers were available (Balzers QMG 111A and Leybold Q-100). One of them could be differentially pumped so that investigations at higher pressures were possible.

The sample was a Pt(100) single crystal of dimensions $7\times7\times1$ mm. It had been oriented to the (100) direction within $\pm$ 0.5° and had been mechanically and electrochemically polished. The crystal was mounted on an L-shaped UHV manipulator allowing translations in three directions and rotations around a vertical and a horizontal axis. It was heated resistively by current passing through two Ta support wires spotwelded to its upper and lower edges. The temperature of the sample was measured by a Ni/NiCr thermocouple spotwelded to its backface. A signal from this thermocouple was also used as feedback input for the heating control unit. In addition, this controller produced the linear temperature ramp in the hysteresis experiments, as well as the periodic modulation of the sample temperature in forcing experiments.

The sample was cleaned by repeated cycles of heating in oxygen ($T\sim900$ K, $p_{O_2}\sim2\times10^{-6}$ mbar), sputtering with Ar ions ($T\sim800$ K, $U_A=800$ V, $p_{Ar}\sim4\times10^{-5}$ mbar), and annealing in UHV up to 1100 K. For the experiments, gases of the highest commercially available purity were used—4.7 for CO, 2.8 for NO (both Linde), 5.0 for O_2, and 5.0 for Ar (both Messer–Griesheim). For steady state measurements and for experiments on kinetic oscillations, the UHV system was used as a constant flow reactor. The pressures of the reactants NO and CO were kept constant using two feedback-stabilized regulation systems for the pressures on the input side of the leak valves leading to the UHV chamber.[19] Each of these control systems consisted of a baratron pressure transducer (MKS 122 A), a magnetic valve (MKS 248 A), and also a turbomolecular pump (50 ℓ/s) for differential pumping through a needle valve. Thus the CO pressure in the main chamber could be kept constant over a long time to within 0.1%, while some drift in p_{NO} was inevitable due to adsorption of NO at the walls of the UHV chamber.

III. EXPERIMENTAL RESULTS

A. Stationary reaction branches and conditions for kinetic oscillations

Kinetic oscillations in the system Pt(100)/NO + CO cannot be established by simply adjusting the partial pressures of p_{NO} and p_{CO} with the sample fixed at a given temperature. Rather, a procedure in which the sample has to be first heated up in the CO + NO mixture above the temperature at which oscillations occur, and then cooled down again, is required. The reason for this, at first sight, peculiar behavior is the existence of two stable stationary branches of the reaction rate. This is illustrated in Fig. 1. Kinetic oscillations can only be obtained on the branch associated with a lowering of the temperature. They exist in two temperature regions of about equal width, but separated by a gap of $\sim$15 K.

A second characteristic feature of the oscillations is that they do not arise spontaneously, but have to be excited by an

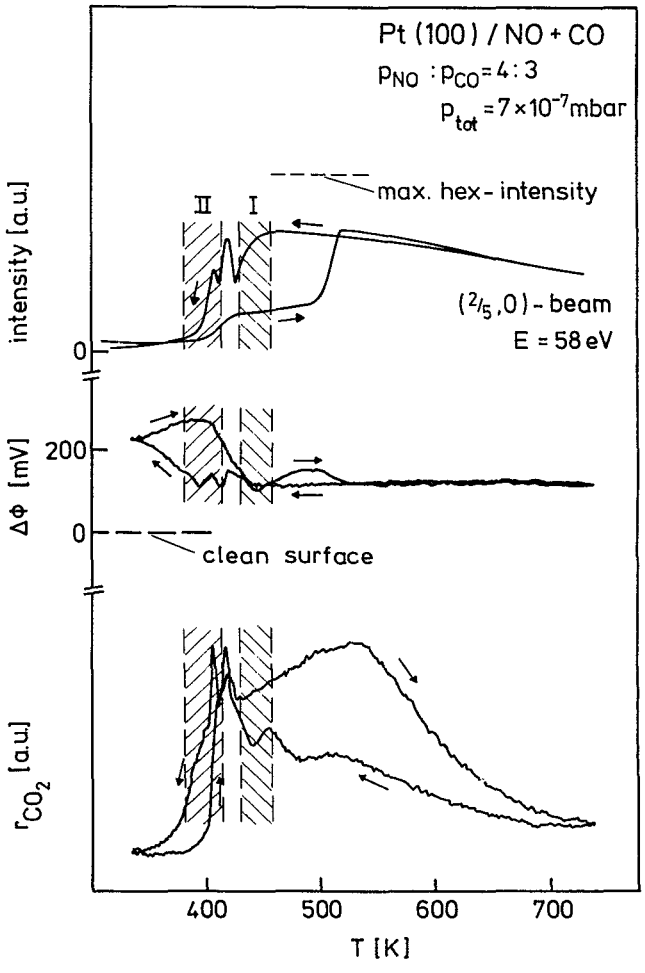

FIG. 1. Hysteresis in reaction rate, work function, and LEED-beam intensity of the hex structure as the temperature is slowly varied in a cycle, while constant NO and CO pressures are maintained. For comparison, the hex intensity that has been measured in pure CO at $T=500$ K and which is almost identical with the hex intensity of the clean reconstructed surface has been marked in the diagram. Apart from some sharp spikes around 400 K which are reproducible, but transient, the curves represent true steady states. Also indicated are the regions where kinetic oscillations have been observed.

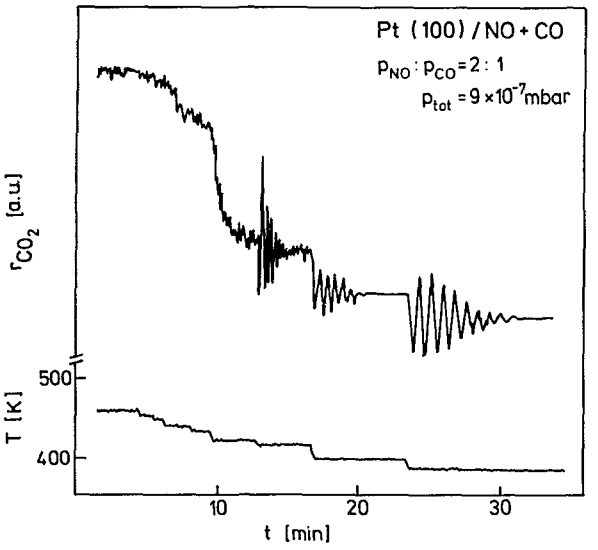

FIG. 2. An example of kinetic oscillations. They can be started by slightly decreasing the temperature and die out after several periods.

initial step down in temperature of a few Kelvin. A typical experimental situation showing the stimulation of kinetic oscillations is depicted in Fig. 2. After each temperature step, the oscillation amplitude decays rapidly within a small number of cycles. The same damping of kinetic oscillations has also been observed by Schmidt *et al.*[6,7] This is seen in the time series published in their reports. They, however, attributed the damping of the oscillations to a progressive contamination of the surface. Contamination as a possible explanation for the damping can be ruled out in our studies for the following reasons:

Experiments carried out on different days demonstrated that the oscillation frequency is reproducible to within a few percent and even the damping characteristics remain approximately the same. Moreover, by applying an external small temperature modulation (>1 K), the damped oscillations can be turned into sustained oscillations. These experiments, which were very reproducible, were extended to a systematic study of the response behavior of the system to periodic and aperiodic perturbations. Results are summarized in a separate paper.[20] Since the properties of the oscillations depend on p_{CO}, p_{NO}, and temperature in a reproducible way, the damping cannot be caused by chemical contaminants. It has to be intrinsic in nature.

Before investigating the properties of the oscillations in more detail, the origin of the hysteresis in the reaction rate visible in Fig. 1 shall be discussed. The existence of multiple branches of the reaction rate is important for an understanding of the oscillations themselves. Apart from some transient fine structures, the two branches of the reaction rate shown in Fig. 1 are both stable above ~ 400 K and therefore mark a true hysteresis. Kinetic effects come into play, however, in the region below ~ 400 K, where the branch exhibiting the lower reaction rate is the only stable one.

The hysteresis in the reaction rate is associated with a hysteresis in the surface structure with the high rate (heating) branch belonging to the 1×1 surface, while the less active (cooling) branch is connected to the hex surface. The phase transition in Fig. 1 was monitored by following the intensity of the LEED $(\frac{2}{3},0)$ beam belonging to the hex phase. The hysteresis in the surface structure shown in Fig. 1 is not very different from the effects observed with each of the gases alone. CO or NO adsorption at low temperature causes a lifting of the hex reconstruction, while desorption at a higher temperature leads to the reappearance of the hex structure.[16,18]

The connection between the $1\times1 \rightleftharpoons$hex phase transition and the existence of two different catalytic activities is consistent with the finding that only the 1×1 surface is active for NO dissociation. The reconstructed surface is quite unreactive for this process.[16,21] This picture is somewhat too simple, however, as it is inconsistent with the experimental experience in two respects. First, one notes that the hysteresis in the reaction rate in Fig. 1 also extends to the temperature range beyond 520 K where the surface is reconstructed in both branches. Second, the reaction rate on the cooling branch in Fig. 1 is much too high to be caused solely by the inactive hex phase. These discrepancies can be explained in the following way.

The relatively high level of catalytic activity on the reconstructed surface can be attributed to structural defects as these are known to facilitate the dissociation of NO.[22] Structural defects are created in the $1\times1 \rightleftharpoons$hex phase transition, since the mass transport of $\sim 20\%$ of the surface atoms associated with this transition will necessarily cause structural imperfections. Their removal requires annealing to high temperature and thus causes the existence of a hysteresis in a temperature cycle. The two branches of the reaction rate in this hysteresis are both associated with a hex surface, but with a different degree of structural perfection. The comparison of the hex intensity in Fig. 1 with the hex intensity in pure CO demonstrates that the intensity of the hex surface in NO + CO remains considerably below the intensity level reached in either pure NO or CO. This difference can only be caused by the surface reaction itself which apparently creates additional surface defects besides the defects formed as a result of the $1\times1 \rightleftharpoons$hex phase transition.

Although the existence of structural defects is important for an understanding of the behavior of the surface reaction above 500 K, their role appears to be of minor importance for the kinetic oscillations. These occur at lower temperature around $T \sim 400$ K and their existence appears to be related to two other phenomena which are found in the same temperature range. First, one notes sharp spikes in the reaction rate in this temperature range. These are reminiscent of the so-called surface explosion. The explosive CO_2 formation evidently takes place also under stationary conditions, and since the two existence regions for kinetic oscillations are located in the same temperature region as that for the explosive reaction, a close connection between both phenomena appears to be obvious.

Second, the two existence ranges for kinetic oscillations in Fig. 1 are located in the vicinity of the CO/NO-induced hex$\rightleftharpoons 1\times1$ phase transition. The adsorbate-induced $1\times1 \rightleftharpoons$hex phase transition has been discussed extensively for the system Pt(100)/CO, where it has been shown to be controlled by critical adsorbate coverages.[18] Under condi-

tions of adsorption/desorption equilibrium, one observes a hysteresis associated with the $1\times1\rightleftharpoons$hex phase transition, since the adsorption energy of CO is ~10 kcal/mol higher on the 1×1 than on the hex phase. A quite similar behavior to that for CO has been found in the NO-induced $1\times1\rightleftharpoons$hex phase transition.[16] The questions are therefore: how does the surface reaction influence the $1\times1\rightleftharpoons$hex phase transition and what role does the phase transition play in the oscillation mechanism?

In order to answer the first part of this question, $\Delta\phi$-hysteresis measurements with each of the pure gases and with reaction mixtures of $p_{NO}/p_{CO}=1{:}1$ and $p_{NO}/p_{CO}=2{:}1$ were carried out. The results are displayed in Fig. 3. The reference level in these measurements is the clean hex surface. CO adsorbed on the 1×1 phase causes a maximum $\Delta\phi$ increase of ~200 mV [Fig. 3(a)], while NO molecularly adsorbed on the 1×1 surface results in a $\Delta\phi$ decrease of ~50 mV below the level of the clean hex surface. The large $\Delta\phi$ increase of ~300 mV that is observed upon heating Pt(100) in an atmosphere of pure NO is due to the dissociation of NO. This takes place on the 1×1 phase above ~380 K [Fig. 3(d)].[16] The nitrogen atoms so formed recombine and desorb quite rapidly (surface residence time <1 s at 400 K) after dissociation.[16] This leaves only atomic oxygen on the surface and the oxygen accumulation is monitored by the rise in $\Delta\phi$. Only in the case of Pt(100)/CO is the width of the $\Delta\phi$ hysteresis identical with the width in the hysteresis of the $1\times1\rightleftharpoons$hex phase transition [Fig. 3(a)]. In the Pt(100)/NO system, the hysteresis in the surface structure is almost the same as with CO, but this similarity is masked

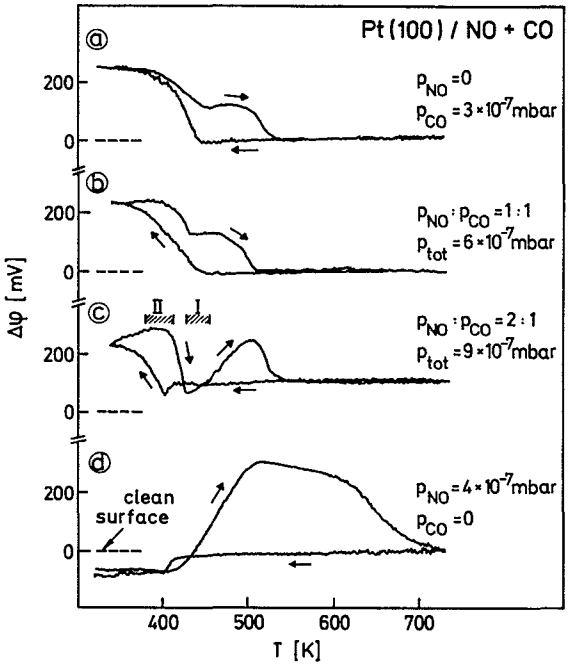

FIG. 3. Hysteresis in the work function during slow cyclic temperature variation for the pure gases (a) CO and (d) NO and also for two different mixtures [(b) and (c)]. With a (c) NO:CO ratio of 2:1, kinetic oscillations can be obtained in the marked regions. The zero level of all curves corresponds to the clean adsorbate-free surface with hexagonal reconstruction.

in the $\Delta\phi$ measurements by the additional effect of NO dissociation [Fig. 3(d)].

Kinetic oscillations in the NO + CO reaction on Pt(100) were obtained for p_{NO}/p_{CO} ratios between 4:3 and 3:1. With a p_{NO}/p_{CO} ratio of 1:1 (which is just outside the oscillatory range), the resulting $\Delta\phi$ hysteresis in Fig. 3(b) is almost identical to that in pure CO. A small downward shift in temperature can be ascribed to the influence of the surface reaction which reduces the CO coverage on the 1×1 phase.

Increasing the p_{NO}/p_{CO} ratio to 2:1, a value inside the oscillatory region, leads to a sharp drop in the $\Delta\phi$ heating curve at ~420 K followed by a relative maximum at ~500 K [Fig. 3(c)]. The formation of the relative $\Delta\phi$ maximum at ~500 K is characteristic for situations where p_{NO}/p_{CO} is inside the oscillatory range of $4{:}3\leqslant p_{NO}/p_{CO}\leqslant3{:}1$. Its appearance is due to the formation of an oxygen covered 1×1 phase above 400 K which, upon further heating, is transformed into the almost adsorbate-free hex phase at $T>520$ K. Apparently the p_{NO}/p_{CO} ratio has to be high enough to allow the buildup of an O adlayer as a necessary prerequisite for the development of kinetic oscillations. The LEED intensities in Fig. 1 indicate that the formation of the oxygen-covered 1×1 surface goes along parallel with the creation of hex islands above 400 K. This is apparently a consequence of the removal of the molecular CO/NO adsorbate. The mechanistic step which leads to the O adlayer is clearly the dissociation of NO on the 1×1 surface. This can be seen from the similar slopes of the $\Delta\phi$ heating curves with pure NO [Fig. 3(d)] and with $p_{NO}/p_{CO}=2{:}1$ [Fig. 3(c)] in the temperature range between 400 and 500 K.

What is also remarkable in this context is the level of the work function that is associated with the hex phase under reaction conditions. As can be seen from Fig. 3(c) the work function is ~100 mV above the level of the clean surface even at high temperature ($T\sim700$ K). The only stable adsorbate on the surface in this temperature range is oxygen. Since the maximum $\Delta\phi$ value of 600 mV occurs for an oxygen coverage of 0.6, one can easily calculate from the $\Delta\phi$ value of about 100 mV a stationary oxygen coverage of about 0.1. This small amount of oxygen remaining permanently on the surface enables the surface reaction to continue even at high temperature and explains the relatively high reaction rate on the cooling branch of the hysteresis. With pure NO, such an offset in the $\Delta\phi$ level with respect to the clean reconstructed surface is not observed. We attribute this difference to defects which are only produced in the NO + CO reaction and which enhance NO decomposition. Therefore no significant stationary oxygen concentration is found if the hex phase is kept at high temperature in a NO atmosphere. The incomplete reconstruction in the LEED hysteresis (Fig. 1) can be attributed to such defects, e.g., 1×1 areas on the surface that are stabilized by adsorbed oxygen.

When the hex phase is cooled down in the pure gases, CO adsorption lifts the hex reconstruction below 430 K. This is indicated by the rise of $\Delta\phi$ [Fig. 3(a)]. With pure NO, the sample has to be cooled further to ~410 K for the NO-induced lifting of the hex reconstruction to occur. Completion of this process is signaled by the beginning of a $\Delta\phi$ decrease[16] [Fig. 3(d)]. It is evident that the NO/CO-in-

duced lifting of the hex reconstruction has to be an essential step in the mechanism of the kinetic oscillations. This can also be seen from the proximity of the two existence regions to the corresponding transition points in the CO and NO hysteresis. It is quite noteworthy that the separation of the two existence regions of ~15 K is about the same as the temperature difference between the CO- and the NO-induced lifting of the hex reconstruction.

The high temperature limit for kinetic oscillations coincides with the beginning of the CO-induced lifting of the hex reconstruction. The upper temperature region (region I) for kinetic oscillations is characterized by the condition that only CO, and not NO adsorption can lift the hex reconstruction. The LEED data in Fig. 1 demonstrate that the reconstruction is only partially lifted in this range. The upper boundary of the lower existence region for kinetic oscillations (region II) is characterized by the condition that both NO and CO can lift the hex reconstruction. How these different conditions lead to different LEED behavior during the kinetic oscillations will be shown in Sec. IIIC, where the results of *in situ* LEED measurements will be discussed.

For a characterization of the kinetics of the NO + CO reaction on Pt(100), p_{CO} in addition to the temperature, has also been varied in a cycle while following the reaction rate and the work function changes. The results displayed in Fig. 4 show that a hysteresis is observed with a cycle time of 10 min. This hysteresis disappears, however, if the variation of p_{CO} is carried out sufficiently slow. In contrast to the real hysteresis which exists if the temperature is varied, only a single stable branch of the reaction is encountered upon variation of p_{CO}. The rate curve in Fig. 4 exhibits a sharp maximum at $p_{NO}/p_{CO} \sim 1{:}1$. The asymmetry in the flanks of the rate maximum demonstrates that the CO adlayer that forms at high p_{CO} is more efficient in inhibiting the surface reaction than is the NO adlayer that exists at low p_{CO}, respectively. The rate maximum appears to be correlated with equal coverages of NO and CO judging from the corresponding $\Delta\phi$ level in Fig. 4.

The large hysteresis effects which are obtained with a cycle time of 10 min demonstrate that at 410 K the reaction approaches its stationary value very slowly. The slowness of this process cannot be attributed to the surface reaction which can still be explosive at $T \sim 400$ K, but is due to a replacement process in which the more stable adlayer CO completely replaces the other adsorbate. With $p_{CO}/p_{NO} > 1$, for instance, one usually obtains a CO-covered surface as the stable final state at $T = 410$ K. Such effects might result from the competitive adsorption/desorption processes between the two gases.

B. Amplitude and frequency of the oscillations

Kinetic oscillations in the system Pt(100) NO + CO do not evolve spontaneously, but have to be stimulated by an initial small temperature step (ΔT) as illustrated by Fig. 2. The initial amplitude of the oscillations which are excited in this way is proportional to the magnitude of ΔT. This relationship is demonstrated by the results in Fig. 5. There the temperature step was realized by rapidly cooling the sample from varying initial temperatures to the same final temperature of $T = 393$ K. The initial amplitude of the rate oscillations is quite high in these experiments and amounts to about 20% of the difference between the two rate branches (see Fig. 1) for a ΔT of 5 K. The method of stimulating kinetic oscillations by a fast parameter change is only successful for temperature variations. Sudden changes in the partial pressures result in a simple relaxation behavior.

Examples of oscillations in the reaction rate and in $\Delta\phi$ are displayed in Fig. 6 for the two existence regions. Oscillations with a measurable variation of $\Delta\phi$ are only found in the lower existence region (region II) where the maximum $\Delta\phi$ amplitude is ~50 mV. In the upper temperature region (re-

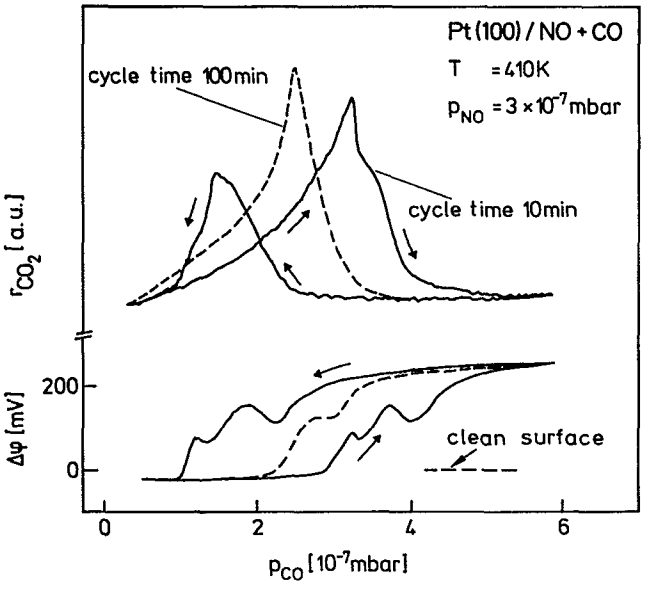

FIG. 4. Hysteresis in the work function and reaction rate upon cyclic variation of the CO pressure, while p_{NO} and the sample temperature are kept constant. The two branches of the reaction coalesce as the cycle time is increased. Thus the hysteresis is only a kinetic phenomenon.

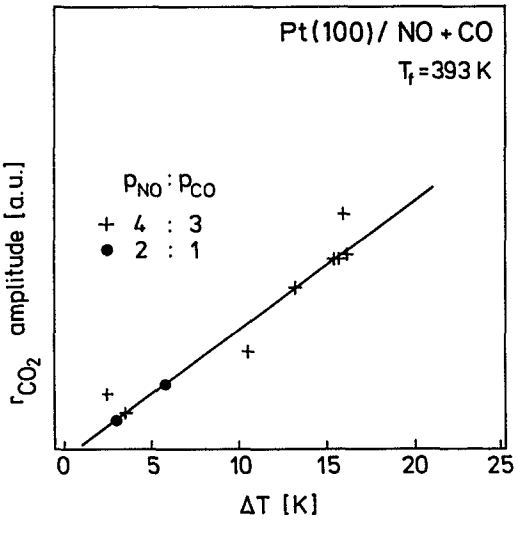

FIG. 5. Influence of the magnitude of the starting temperature step on the amplitude of kinetic oscillations. The final temperature T_f of the sample was kept constant, while the starting value was varied.

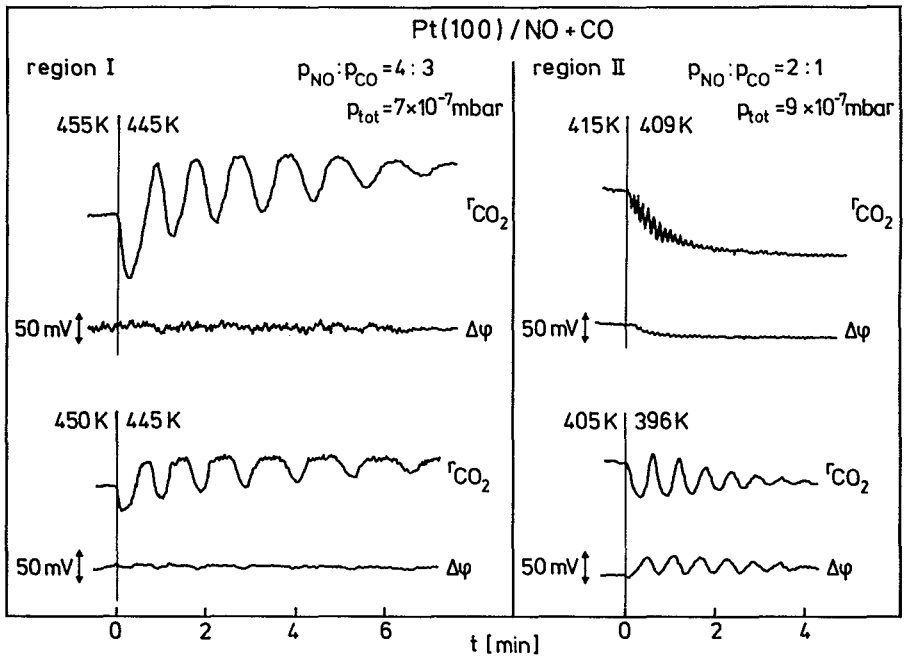

FIG. 6. Examples of kinetic oscillations in the two existence regions marked in Fig. 1.

gion I), the adsorbate coverages are apparently very low, since $\Delta\phi$ exhibits an almost constant value there. The same conclusions were also drawn by Schmidt *et al.* who performed measurements with Auger electron spectroscopy.[6,7]

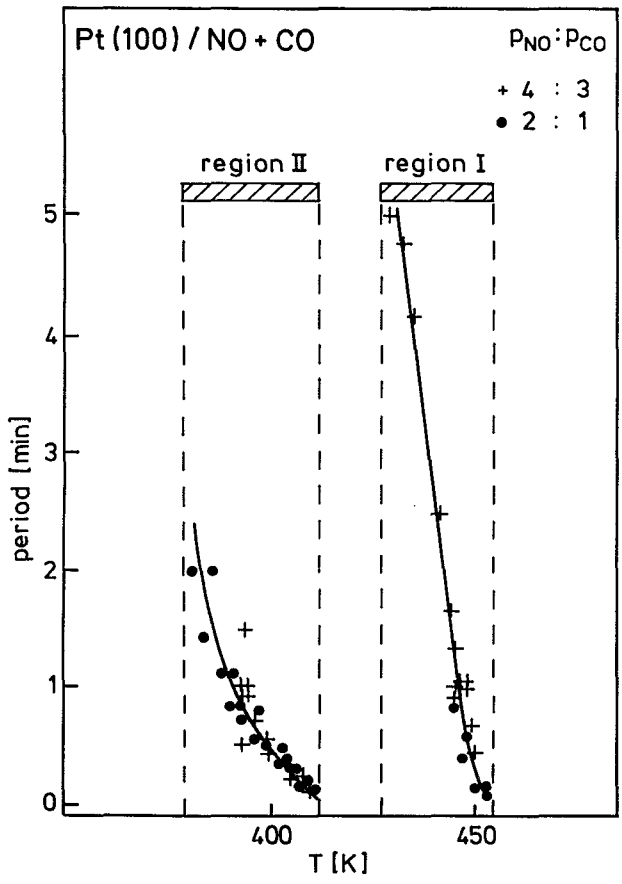

FIG. 7. Dependence of oscillation period on sample temperature. Most data in region I have been obtained for a $p_{NO}:p_{CO}$ ratio of 4:3 and for a corresponding ratio of 2:1 in region II. The total pressures were 7×10^{-7} mbar (4:3) and 9×10^{-7} mbar (2:1).

The oscillations are mostly of sinusoidal shape, but relaxation like oscillations are observed as well. After excitation, the oscillations in $\Delta\phi$ and in the reaction rate in region II start with an initial phase difference of 180°, but within the following cycle, the phase difference changes to 90° and then remains constant. This relationship between the rate and the $\Delta\phi$ oscillations is very reproducible and holds for the existence region II.

Experiments with varying p_{NO}/p_{CO} ratios showed that the period of the oscillations is very insensitive to variations in p_{NO}/p_{CO}, but reacts sensitively to a change in temperature. This behavior is shown in Fig. 7, where the oscillation period has been plotted as a function of temperature for two different p_{NO}/p_{CO} ratios 4:3 and 2:1 in the two existence regions for kinetic oscillations. One notes that neither the existence regions nor the oscillation periods exhibit a pronounced dependence on the p_{NO}/p_{CO} ratio.

For both regions, the dependence of the oscillation period on temperature is qualitatively similar. When the respective region is reached for the high temperature side, oscillations start with fairly small periods which continuously increase with decreases in T. They eventually tend toward infinity as the lower boundary of the existence region is approached. Although these effects are partly masked by the damped character of the oscillations, they suggest the occurrence of homoclinic bifurcations. This interpretation is supported by the results of the mathematical modeling given below.

C. LEED observations during kinetic oscillations

With the system Pt(100)/CO + O_2, it has been possible to verify directly the participation of the $1\times1\rightleftharpoons$hex phase transition in the kinetic oscillation mechanism by demonstrating that the oscillations in the reaction rate are accompanied by periodic variations in the LEED intensity of the hex structure.[12] Such *in situ* measurements were also carried

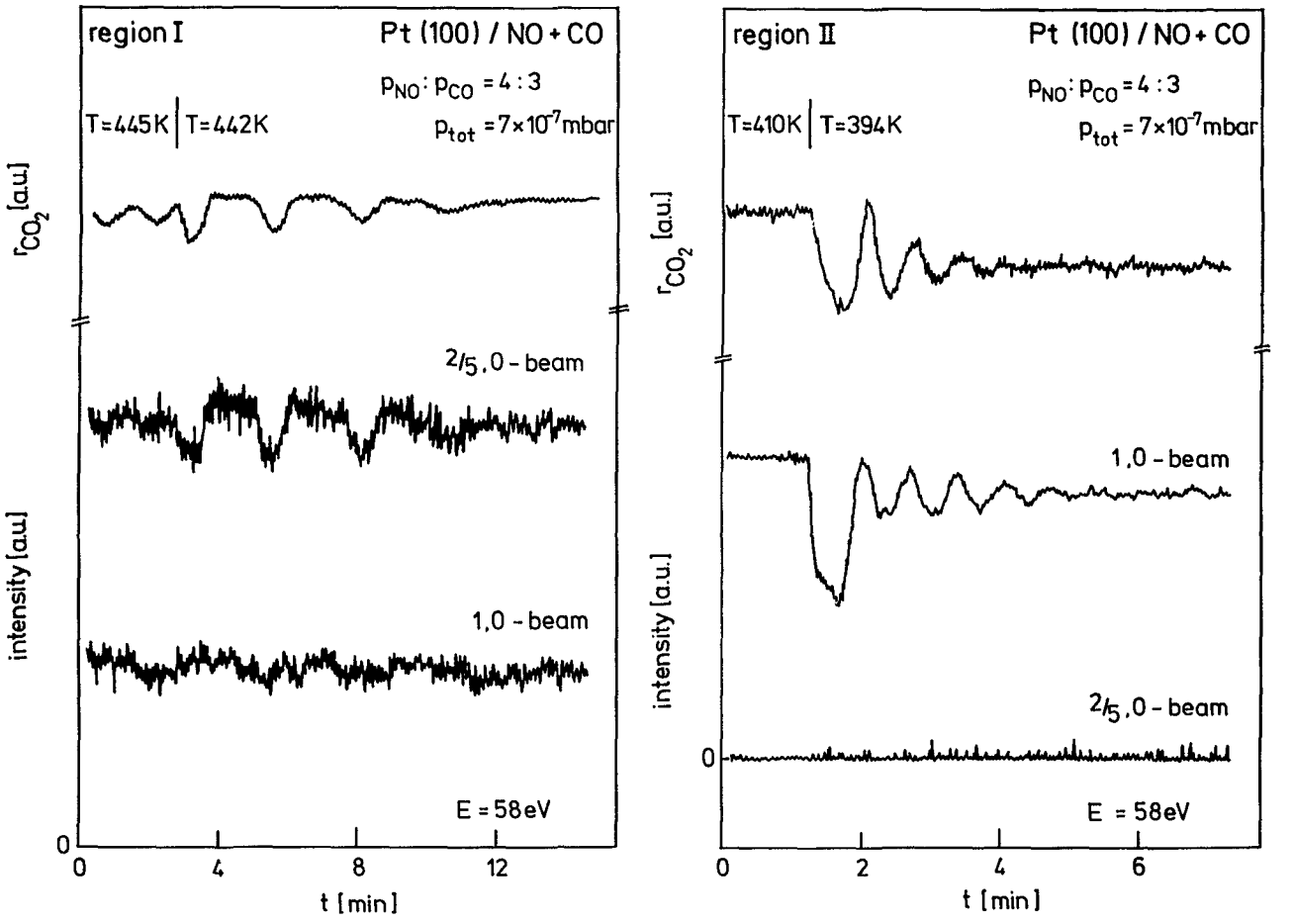

FIG. 8. Changes in surface structure during kinetic oscillations as monitored by video LEED. (a) *Region I*: Changes in hex structure intensity occur in parallel to the reaction rate oscillations indicating the participation of the hex$\rightleftharpoons 1\times 1$ phase transition in the oscillation mechanism. (b) *Region II*: The LEED intensity of hex structure beams is always zero; hence the phase transition hex$\rightleftharpoons 1\times 1$ is not involved in the mechanism of oscillations.

out with the present system during kinetic oscillations. The results displayed in Fig. 8, reveal a qualitatively different picture for each of the two existence regions. In region I, at higher temperature, the system behaves similarly to Pt(100)/CO + O_2. The oscillations in the reaction rate are accompanied by corresponding oscillations in the LEED intensities such that the maxima in the reaction rate coincide with the maxima in the hex intensity. As demonstrated by the small modulation of the hex intensity in Fig. 8(a), however, only a small fraction of the surface undergoes the $1\times 1\rightleftharpoons$hex phase transition, while the rest remains in the hex state all the time. The small amplitude of the hex intensity oscillations is consistent with the amplitude of the rate oscillations which is, likewise, relatively small and with the small coverage variations indicated by the $\Delta\phi$ measurements.

The seemingly obvious conclusion that the kinetic oscillations in the NO + CO reaction are linked to the $1\times 1\rightleftharpoons$hex phase transition does no longer hold for region II, however [Fig. 8(b)]. The kinetic oscillations here proceed on a surface which does not exhibit any intensity in the position of the hex beams. The surface remains in the 1×1 state all the time. The large oscillations in the intensity of the integral order beams can be attributed simply to variations in the adsorbate coverages. This is in agreement with the work function measurements in Fig. 6 which likewise indicate considerable coverage changes.

As discussed above, kinetic oscillations in the upper temperature range proceed under conditions where only CO adsorption, but not NO adsorption, can lift the reconstruction. This condition leads to a surface which is largely reconstructed. The surface reaction between CO and NO apparently keeps the CO + NO coverage low and thereby preventing the complete lifting of the hex reconstruction. The small variations in the hex intensity which are observed in region I have to be ascribed to changes in CO and NO coverages which modulate the size of the 1×1 area. This may happen in a cycle whereby CO adsorption causes the formation of 1×1 islands which then relax back into the hex structure as NO coadsorbs and reacts off with the CO.

The condition that both NO and CO can lift the hex reconstruction is evidently responsible for the complete disappearance of the hex structure in the lower temperature region of kinetic oscillations. Since oscillations in this region arise on a surface which remains entirely in a 1×1 state, it is clear that the $1\times 1\rightleftharpoons$hex phase transition cannot be essential for kinetic oscillations. It is rather unlikely that two different mechanisms for kinetic oscillations exist within one system. Therefore the primary aim below will be to look for a mecha-

nism that is not based primarily on the $1\times1\rightleftharpoons$hex phase transition. This mechanism will be outlined in the following section where a mathematical model for the NO + CO reaction on Pt(100) is presented.

IV. MATHEMATICAL MODELING

A. The model

The model of the surface reaction that is presented here for explaining kinetic oscillations is identical to that which had been successfully employed in a previous modeling of the explosive product formation observed in TPR experiments with coadsorbed CO and NO on Pt(100).[16] For a consistent modeling of the NO + CO reaction on Pt(100), it is required that the surface explosion as well as the kinetic oscillations be reproduced with the same set of differential equations (DE's) using the same values for the rate parameters.

We assume that the surface reaction between NO and CO proceeds via the dissociation of adsorbed NO and formulate the individual reaction steps as follows:

$$CO + * \leftrightarrows CO_{ad}, \quad (R1)$$

$$NO + * \leftrightarrows NO_{ad}, \quad (R2)$$

$$NO_{ad} + * \rightarrow N_{ad} + O_{ad}, \quad (R3)$$

$$2N_{ad} \rightarrow N_2 + 2*, \quad (R4)$$

$$CO_{ad} + O_{ad} \rightarrow CO_2 + 2* \quad (R5)$$

(* denotes a free adsorption site). The formation of N_2O from adsorbed NO and N as a side product of the NO + CO reaction has been investigated by several authors on polycrystalline Pt under various conditions. At low pressure, N_2O production was never found to be more than a few percent of the main reaction products CO_2 and N_2.[23,24] It is also known that adsorbed N_2O is stable only below room temperature.[25,26] Therefore a large influence of N_2O on the main reaction, e.g., in removing NO_{ad} or in blocking adsorption sites, can be ruled out and N_2O can be neglected in our reaction scheme.

The rate-limiting step in the sequence above is the dissociation of NO. According to reaction (R3), this requires a free adsorption site. Since the number of vacant adsorption sites increases in the subsequent reaction steps (R4) and (R5), the kinetics of the surface reaction described by steps (R3), (R4), and (R5) exhibit an autocatalytic behavior

$$NO_{ad} + CO_{ad} + * \rightarrow CO_2 + 1/2\ N_2 + 3*. \quad (R3 + 0.5\cdot R4 + R5)$$

The autocatalysis which is provided by the vacant site requirement for NO dissociation has been shown to be primarily responsible for the explosive surface reaction between coadsorbed NO and CO.[15,16]

The $1\times1\rightleftharpoons$hex phase transition influences the surface reaction only indirectly in that it leads to the formation of mixed 1×1-NO/CO islands within which the surface reaction proceeds. Since the *local* coverage in the 1×1 islands of about 0.5 is independent of the CO/NO exposure up to the complete lifting of the hex reconstruction at $\theta_{CO,NO} = 0.5$, the position and the sharpness of the autocatalytic CO_2 and N_2 product peaks are found to be independent of the *total* coverage (up to $\theta = 0.5$). This is what was observed in the experiment.[13–16]

The driving force for the formation of mixed 1×1 islands is the gain in adsorption energy that results from such a formation. The adsorption energy on the 1×1 phase has been shown to be substantially higher than on the hex phase for both gases.[16,18] Experimentally, the formation of mixed 1×1-NO/CO islands has been deduced from the results of vibrational spectroscopy which showed that the stretching frequencies for CO and NO were lower in their coadsorbed state than for each adsorbate alone.[13]

In our model, the surface reaction between NO and CO is therefore completely restricted to the 1×1 area. The hex phase is assumed to be inactive for NO dissociation. The $1\times1\rightleftharpoons$hex phase transition only regulates the proportion of the surface area that is active. The mechanism, the kinetics, and the energetics of the adsorbate-induced $1\times1\rightleftharpoons$hex phase transition are well known from previous investigations.[16,18,27,28] The phase transition in both directions is controlled by critical adsorbate coverages. The hex reconstruction is lifted as soon as the coverage exceeds a critical value and a relaxation of the 1×1 surface into the reconstructed hex state takes place as the adsorbate coverage drops below a second lower critical limit.

The starting point of the mathematical treatment was a set of coupled DE's developed originally to describe kinetic oscillations which occur in the system Pt(100)/CO + O_2 as consequence of the $1\times1\rightleftharpoons$hex phase transition.[11] This system of DE's had to be modified to the reaction sequence (R1)–(R5) in order to include the dissociation of NO which now supplies the atomic oxygen needed for CO oxidation. The influence of NO on the phase transition and the adsorption/desorption behavior of NO on the two surface phases are treated in the same way as for CO. Furthermore, we assume that the kinetic oscillations proceed under isothermal conditions on a spatially homogeneous surface. We neglect the influence of small variations in p_{NO} and p_{CO} due to mass balance in the reaction and set the partial pressures of the reactants as being constant.

Starting with the Pt(100)/CO + O_2 model, one arrives first at a set of six coupled DE's which describe the variation of the CO and NO coverages on the two surface phases ($\theta_{CO}^{1\times1}$, θ_{CO}^{hex}, $\theta_{NO}^{1\times1}$, θ_{NO}^{hex}), the change in the oxygen coverage on the 1×1 phase ($\theta_O^{1\times1}$), and the fraction of the surface which is present as 1×1 phase ($\theta_{1\times1}$) with $\theta_{1\times1} + \theta_{hex} = 1$. The adsorbate coverages in the equations all refer to the total number of sites (hex + 1×1) and have to be divided by $\theta_{1\times1}$ in order to obtain the *local* coverages in the 1×1 islands.

$$\frac{d\theta_{CO}^{1\times1}}{dt} = k_1 p_{CO}\theta_{1\times1}\left(1 - \frac{\theta_{CO}^{1\times1}}{\theta_{1\times1}} - \frac{\theta_{NO}^{1\times1}}{\theta_{1\times1}}\right) - k_2\theta_{CO}^{1\times1} + k_3\theta_{1\times1}\theta_{CO}^{hex} - k_4\frac{\theta_{CO}^{1\times1}\theta_O^{1\times1}}{\theta_{1\times1}}, \quad (I)$$

$$\frac{d\theta_{CO}^{hex}}{dt} = k_1 p_{CO}\theta_{hex} - k_5\theta_{CO}^{hex} - k_3\theta_{1\times1}\theta_{CO}^{hex}, \quad (II)$$

$$\frac{d\theta_{NO}^{1\times1}}{dt} = k_1 p_{NO}\theta_{1\times1}\left(1-\frac{\theta_{CO}^{1\times1}}{\theta_{1\times1}}-\frac{\theta_{NO}^{1\times1}}{\theta_{1\times1}}\right)-k_6\theta_{NO}^{1\times1}+k_7\theta_{1\times1}\theta_{NO}^{hex}-k_8\frac{\theta_{NO}^{1\times1}\theta_{empty}^{1\times1}}{\theta_{1\times1}}, \tag{III}$$

$$\frac{d\theta_{NO}^{hex}}{dt} = k_1 p_{NO}\theta_{hex}-k_9\theta_{NO}^{hex}-k_7\theta_{1\times1}\theta_{NO}^{hex}, \tag{IV}$$

$$\frac{d\theta_{O}^{1\times1}}{dt} = k_8\frac{\theta_{NO}^{1\times1}\theta_{empty}^{1\times1}}{\theta_{1\times1}}-k_4\frac{\theta_{CO}^{1\times1}\theta_{O}^{1\times1}}{\theta_{1\times1}}, \tag{V}$$

$$\frac{d\theta_{1\times1}}{dt} = \begin{cases} \dfrac{\dot\theta_{CO}^{1\times1}+\dot\theta_{NO}^{1\times1}}{\theta_{grow}^{1\times1}}, & \text{if } \dot\theta_{CO}^{1\times1}+\dot\theta_{NO}^{1\times1}>0 \text{ and } \dfrac{\theta_{CO}^{1\times1}+\theta_{NO}^{1\times1}}{\theta_{1\times1}}>\theta_{grow}^{1\times1} \\ -k_{10}(\theta_{1\times1}-\theta_{def}\theta_{hex})(1-c), & \text{if } c\leqslant 1 \text{ and } \theta_{1\times1}\geqslant\theta_{def}\theta_{hex} \\ 0, & \text{otherwise,} \end{cases} \tag{VI}$$

where

$$c=\frac{\theta_{CO}^{1\times1}+\theta_{NO}^{1\times1}}{\theta_{1\times1}\theta_{CO,NO}^{crit}}+\frac{\theta_{O}^{1\times1}}{\theta_{1\times1}\theta_{O}^{crit}}$$

and

$$\theta_{empty}^{1\times1}=\max\left[\left(\theta_{1\times1}-\frac{\theta_{NO}^{1\times1}+\theta_{CO}^{1\times1}}{\theta_{CO,NO}^{inh}}-\frac{\theta_{O}^{1\times1}}{\theta_{O}^{inh}}\right),\ \theta_{def}^{free}\right],$$

with

$$\theta_{def}^{free}=\max\left[(\theta_{def}\theta_{1\times1}-\theta_{O}^{1\times1}),\ 0\right].$$

The influence of chemisorbed nitrogen has been completely neglected here, since it has been demonstrated in a previous calculation with an extended set of DE's that the presence of atomic nitrogen has only a small influence on the surface reaction.[16] Above room temperature, the nitrogen atoms formed by dissociation of NO recombine and desorb practically instantaneously.

For the adsorption of NO and CO on the two surface phases (k_1), simply Langmuirian kinetics was applied assuming that sites are blocked only by adsorbed CO and NO, but not by adsorbed oxygen. For CO/NO adsorption onto the hex phase, any coverage dependence of the adsorption rate has been neglected. This is because the coverages on this phase are very small. For all adsorption parameters, the same constant k_1 has been used. This is reasonable as the initial sticking coefficient has been shown to be close to one for both gases and for both surface phases.[16,18,21] The desorption parameters (k_2, k_5, k_6, k_9) contain the energetics of CO/NO desorption on the two surface phases. The higher adsorption energy of CO and NO on the 1×1 phase leads to a correspondingly smaller desorption rate (see Table I). Consequently, the equilibrium coverages of CO and NO on the 1×1 phase are substantially higher than on the hex phase.

In our model, both the NO dissociation and the surface reaction to form CO_2 are entirely restricted to the 1×1 phase. According to reaction step (R3), the rate of NO dissociation in the term containing k_8 is set proportional to the NO coverage $\theta_{NO}^{1\times1}$ and to the concentration of vacant 1×1 sites $\theta_{empty}^{1\times1}$. Since we know from experiment the coverages at which the dissociation of NO is completely inhibited, the vacant site concentration $\theta_{empty}^{1\times1}$ can be calculated for given adsorbate coverages. The inhibition coverages which had been used are $\theta_{CO,NO}^{inh}\approx0.5$ for adsorbed CO and NO and $\theta_{O}^{inh}\approx0.4$ for adsorbed oxygen.[16]

The hysteresis data displayed in Fig. 1 have shown that even the reconstructed surface exhibits a considerable level of catalytic activity. This effect has been attributed to structural defects which because of their strong influence on the reaction have also been included in our model. A certain fraction of the surface θ_{def}, is assumed to be in a quasi-"1×1" state which does not participate in the $1\times1\rightarrow$hex phase transition and which, therefore, remains active all the time. In addition, a higher catalytic activity in NO dissociation is assigned to those defect sites which lie in 1×1 areas by considering them as additional vacant sites. In the DE's, these defects influence the catalytic activity via the calculational scheme for $\theta_{empty}^{1\times1}$.

For reasons of internal consistency, the oxygen which is formed through the dissociation of NO at defect sites had to be assumed to remain fixed, thereby blocking these sites for the further dissociation of NO. The number of free defect sites is termed as θ_{def}^{free} in the formulas. This means that the defect sites become active only below a certain oxygen coverage. This coverage is equal to the saturation oxygen coverage of the defect sites. We further assume that the defect sites are homogeneously distributed over the entire surface. The fraction of the defects that is located in the 1×1 area and is contributing only to the surface reaction in our model is then equal to $\theta_{def}\cdot\theta_{1\times1}$. The contribution of all other defects which are located in the reconstructed area is neglected for NO dissociation and in the surface reaction. These local reaction centers are isolated and have no influence on the reaction in the 1×1 islands.

The treatment of the adsorbate-induced $1\times1\rightleftharpoons$hex phase transition is identical to that of the mathematical model used for kinetic oscillations in the Pt(100)/CO + O_2 system.[11] Since both gases NO and CO exhibit the same behavior with respect to the phase transition, no differentiation has been made in the mathematical model in their influence towards the phase transition.

The lifting of the hex reconstruction proceeds through the growth of 1×1-NO/CO islands. Here also structural defects play an important role, since they act as nucleation centers for the hex$\rightarrow1\times1$ phase transition. In this process,

TABLE I. Temperature-dependent parameters used for the simulation of the NO + CO reaction on Pt(100).

Description	Parameter	E^*(kcal/mol)	$\nu(s^{-1})$	Value at 400 K	References
CO desorption 1×1	k_2	37.5 ($\theta=0$)	1.0×10^{14}	3.1×10^{-7}	18
		36.4 ($\theta=0.3$)	1.0×10^{14}	1.2×10^{-6}	
		34.5 ($\theta=0.5$)	1.0×10^{14}	1.4×10^{-5}	
CO desorption hex	k_5	27.5	4.0×10^{12}	3.7×10^{-3}	18
NO desorption 1×1	k_6	37.0 ($\theta=0$)	1.7×10^{14}	1.0×10^{-6}	31
		35.9 ($\theta=0.3$)	1.7×10^{14}	4.0×10^{-6}	
		34.0 ($\theta=0.5$)	1.7×10^{14}	4.4×10^{-5}	
NO desorption hex	k_9	26.0	4.0×10^{12}	2.4×10^{-2}	16
NO dissociation	k_8	28.5	2.0×10^{15}	0.52	16
$CO_{ad}+O_{ad}$ reaction	k_4	14.0	2.0×10^{8}	4.4	32
Phase transition 1×1→ hex	k_{10}	25	2.5×10^{10}	5.3×10^{-4}	27, 28
NO/CO trapping on 1×1	k_3, k_7	8.0	2.2×10^{4}	0.93	11

only defects in the hex area are involved and therefore their number is $\theta_{def}\cdot\theta_{hex}$. Starting from such quasi-"1×1" defects, islands of NO/CO will form by trapping CO and NO from the surrounding hex area. These 1×1 islands then grow proportionally to the number of trapped NO/CO molecules. Thus the hex→1×1 phase transition proceeds via 1×1-NO/CO islands. These just grow in size while maintaining a constant local coverage $\theta^{1\times1}_{grow}$ of ~0.5. Only after the complete lifting of the hex reconstruction at $\theta^{1\times1}_{CO}+\theta^{1\times1}_{NO}=0.5$ can the local coverage in the 1×1-NO/CO islands exceed 0.5. The unidirectional diffusion of CO/NO adsorbed on the hex phase to 1×1 areas proceeds in the so-called "trapping" terms (k_3, k_7), where the number of trapped molecules is set proportional to the 1×1 area $\theta_{1\times1}$ and to the number of CO/NO molecules adsorbed on the hex phase.

The phase transition in the direction 1×1→hex proceeds as soon as the adsorbate coverage falls below the critical level that is necessary to stabilize the 1×1 phase. Since all three adsorbates CO, NO, and oxygen stabilize the 1×1 phase, one has to calculate their combined influence on the 1×1→hex phase transition by taking their different critical coverages into account. These are $\theta^{crit}_{CO,NO}\approx0.3$ for CO and NO and $\theta^{crit}_{O}\approx0.4$ for oxygen, respectively.[18,29] With c denoting the 1×1 area stabilized by adsorbate, the metastable 1×1 area that is able to reconstruct is then equal to 1-c. In contrast to the CO/NO-induced hex→1×1 phase transition, which is only weakly activated and even proceeds at 100 K, the transition in the direction 1×1→hex (k_{10}) is strongly activated by about 25 kcal/mol.[27,28,30]

The constants used in the simulation are summarized in Tables I and II. With very few exceptions, all parameters were taken directly from experimental data. The exceptions could be approximated by fitting the simulated curves to experimental data. Since repulsive interactions between adsorbed CO/NO molecules lead to a strong enhancement of CO/NO desorption at higher coverages, the coverage dependence of the adsorption energies of these two gases had to be taken into account in order to keep the simulation as realistic as possible.[18,33,34] In Sec. IVD, it will be shown that this is a necessary condition for the occurrence of kinetic oscillations. Using experimental data which have been determined for Pt(100)/CO, the coverage dependence of the adsorption energy $E_{ad}(\theta)$ can be approximated by a quadratic expression

$$E_{ad}(\theta)=E_{ad}(0)-k_{11}\cdot\theta^2.$$

From TDS data of coadsorbed NO and CO on Pt(111), it is known that the repulsive interactions between molecules in pure CO and pure NO islands and in the mixed NO/CO phase are not identical.[34] It is, however, quite difficult to take these differences into account. We therefore treat them as identical in the model. This simplification can be expected to cause only some deviations with respect to the quantitative

TABLE II. Temperature-independent parameters used for the simulation of the NO + CO reaction on Pt(100).

Description	Parameter	Value	References
NO/CO adsorption:	k_1	2.21×10^5 ML mbar^{-1} s^{-1}	Calculated
Fit parameter for $E^{NO,CO}_{ad}(\theta)$	k_{11}	24 kcal/mol	This work
Inhibition coverages	$\theta^{inh}_{CO,NO}$	0.61	This work
for NO dissociation	θ^{inh}_{O}	0.399	16
Critical coverages for	$\theta^{crit}_{CO,NO}$	0.3	18
phase transition 1×1→hex	θ^{crit}_{O}	0.4	29
Critical NO + CO coverage for 1×1 island growth	$\theta^{1\times1}_{grow}$	0.5	18
Amount of surface defects	θ_{def}	0.0001	This work

behavior of the model, but it will not change its principle features. The coverage dependence of the adsorption energies for CO and NO can be fitted with the same fit parameter k_{12}. The coverage θ then denotes a combined local coverage according to

$$\theta = \frac{\theta_{NO}^{1\times1} + \theta_{CO}^{1\times1}}{\theta_{1\times1}}.$$

B. Simulation with the realistic model

As a first test of the model, a simulation of the hysteresis effects observed in adsorption/desorption equilibrium was carried out. This hysteresis occurs upon cyclic variation of the sample temperature while maintaining an atmosphere of pure CO or NO. The temperature gap between the two existence regions for kinetic oscillations coincides with the separation in transition temperatures for the CO- and NO-induced lifting of the hex reconstruction. This remarkable occurrence suggests that the hysteresis effects are of decisive importance for the kinetic oscillations. Evidently therefore, the parameters which determine the hysteresis behavior for the pure gases first have to be determined as precisely as possible before one can start to simulate the reaction between the two gases.

The results of fitting the simulated hysteresis loops of Pt(100)/CO and Pt(100)/NO to the experimental curves, published in previous work,[16,18] are displayed in Fig. 9. The processes which are important for the hysteresis are the different adsorption/desorption equilibria on the two surface phases (k_1, k_2, k_5, k_6, k_9); the unidirectional diffusion of the adsorbate from the hex to the 1×1 phase in the "trapping" terms (k_3, k_7) and the kinetics of the $1\times1\rightarrow$hex phase transition (k_{10}, $\theta_{CO,NO}^{crit}$). For the Pt(100)/CO system, all parameters were known from experiment with the exception of the trapping constant k_3. This constant had to be determined by a fitting procedure. For Pt(100)/NO, the desorption parameters for the hex phase, in addition to the trapping constant k_7, had also not been determined experimentally. The same trapping constant was chosen for this system as for CO, but for the adsorption energy of NO on the hex phase a lower value was taken than for CO (see Table I). In this way, the hex$\rightarrow1\times1$ transition temperature in pure NO could be shifted downward by 15 K with respect to the corresponding transition temperature for CO. This is what is found from experimental evidence.[16]

Next a simulation of the hysteresis in reaction rate, observed under stationary conditions in the presence of both gases, was carried out. The partial pressures p_{NO} and p_{CO} were held constant, while the sample temperature was varied in a cycle. The simulated rate curve is displayed in Fig. 10. This exhibits a broad hysteresis region which is associated with a similar hysteresis in the surface structure. The experimental results in Fig. 1 show, in principle, the same behavior. Furthermore, as one takes a closer look, one realizes that not only the gross features, but also many of the finer details are reproduced in the simulation. These will be discussed below, together with the kinetic oscillations which also appear during the temperature scans.

Starting at low temperature in Fig. 10, the reaction is inhibited due to high adsorbate coverages, but upon heating, the reaction sets in producing a sharp spike in the reaction rate at 420 K. With increasing temperature, the rate remains at a high level, as the oxygen coverage rises continuously.

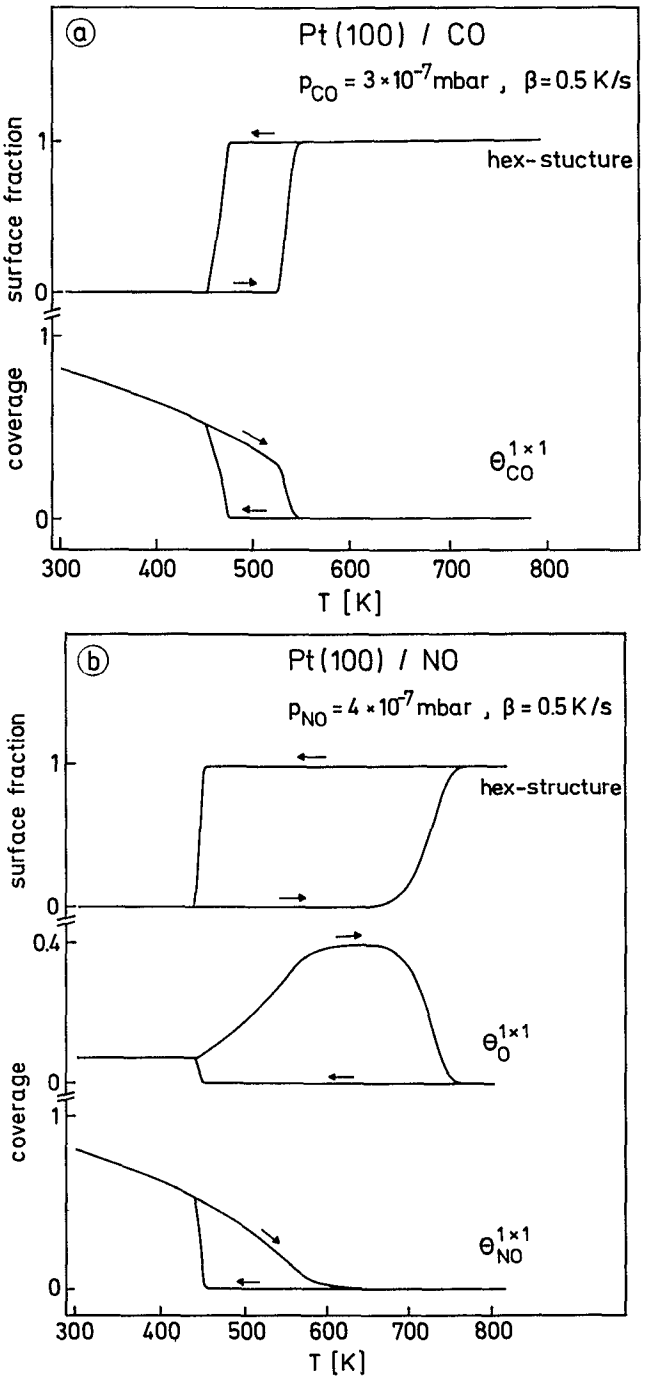

FIG. 9. Model calculation of hysteresis effects in adsorption/desorption equilibrium with the pure gases CO and NO upon cyclic temperature variation. (a) *CO*: The CO coverage on 1×1 ($\hat{=}$ work function) and the amount of hex reconstructed surface show the same hysteresis behavior as observed experimentally [cf. Fig. 3(a) and Ref. 16]. (b) *NO*: The oxygen atoms formed by NO dissociation are removed by thermal desorption. Second order kinetics with an activation energy of 52.1 kcal/mol and a frequency factor of 3×10^{14} s^{-1} were assumed. Displayed are the NO and the oxygen coverages ($\hat{=}$ work function) and on the 1×1 phase, the changes in surface structure. The broad hysteresis in the hex reconstruction is due to atomic oxygen which stabilizes 1×1 areas until the desorption temperature for oxygen is reached [cf. Fig. 3(d) and Ref. 16].

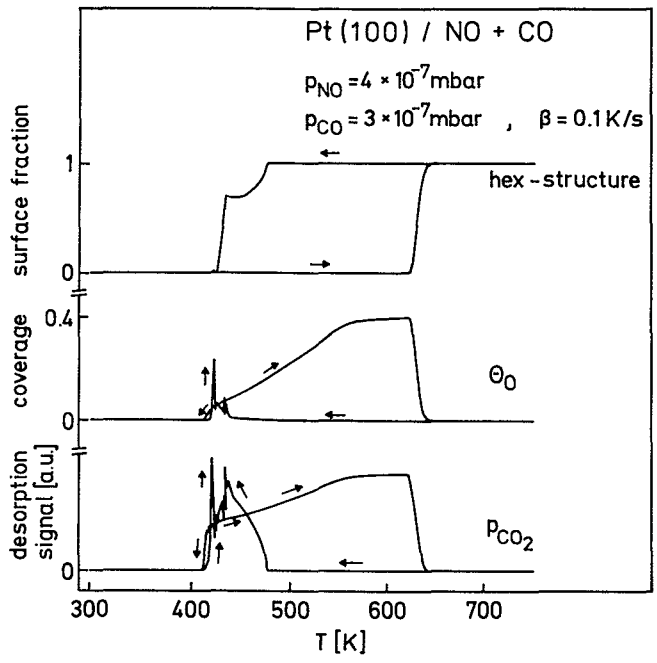

FIG. 10. Model calculation of hysteresis effects in CO_2 production, oxygen coverage ($\triangleq \Delta\phi$ for $T > 400$ K) and the fraction of the surface that is present in the hex structure. The corresponding experimental data are displayed in Fig. 1.

During this time the surface remains in a 1×1 state, but at 620 K, the $1\times1 \rightarrow$ hex phase transition occurs. Simultaneously the oxygen coverage and the reaction rate drop to a value close to zero. During the cooling period, the surface maintains the inactive hex state down to ~480 K, where CO adsorption initiates the hex $\rightarrow 1\times1$ phase transition. This causes the reaction rate to rise again to a high level. Finally, below 410 K, a high adsorbate coverage inhibits the surface reaction.

There are several significant differences in the simulation in comparison with the experiment. These are, however, mainly quantitative in nature. The most pronounced difference is clearly the much wider hysteresis found for the $1\times1 \rightleftharpoons$ hex transition of the simulation. This discrepancy is due to the fact that oxygen desorption was not included in the DE's in an effort to limit their complexity. At intermediate heating rates, in thermal desorption spectra following pure NO exposures, oxygen recombines and desorbs between 600 and 700 K.[16] Under nearly isothermal conditions, as in the simulation, O_2 desorption should occur at lower temperatures. This reduces the coverage and enables the $1\times1 \rightarrow$ hex phase transition to occur at a lower temperature. Qualitatively, the behavior of the model is correct. As in the experiment, a high oxygen coverage is obtained in the heating part of the hysteresis cycle. This is indicated by the relative $\Delta\phi$ maximum at ~500 K in Fig. 1.

The second major difference between simulation and experiment is that in the simulation, the catalytic activity almost ceases with the formation of the hex structure. In the experiment, on the other hand, the CO_2 production rate is still appreciably high on the reconstructed surface. This difference is due to the fact that our model neglects the contribution to the reaction from isolated defect centers on the hex phase. In this respect, it takes into account only the defects located on the 1×1 surface area. Therefore the hex phase does not contribute to the CO_2 production in our model.

As the Pt(100) surface is cooled down in CO/NO, one observes the same stepwise lifting of the hex reconstruction that is displayed in the experimental LEED curve in Fig. 1. Most importantly, one also finds in the simulation kinetic oscillations occurring for the most part only in the cooling part of the temperature cycle. The exception to this is in region III, which is explained in detail below. The amplitude of the oscillations is indicated in Fig. 11. This figure represents the steady states in an expanded section of the cooling branch of the hysteresis cycle of Fig. 10.

In Fig. 11, one can distinguish among three distinct existence regions for kinetic oscillations. These are denoted by I, II, and III. Their separation is due to the stepwise lifting of the hex reconstruction in the cooling part of the temperature cycle. In region I, the conditions for the phase transition are such that only CO adsorption, but not NO adsorption, can lift the hex reconstruction. As found in the experiment, the hex reconstruction is only partially removed in this region, while the surface remains largely in the hex state. As the temperature is decreased further, one enters the region where both NO and CO can lift the hex reconstruction. In agreement with the experimental situation, one observes here the complete removal of the hex reconstruction. The oscillatory region II is located at the beginning of the complete lifting of the hex reconstruction, while the oscillations

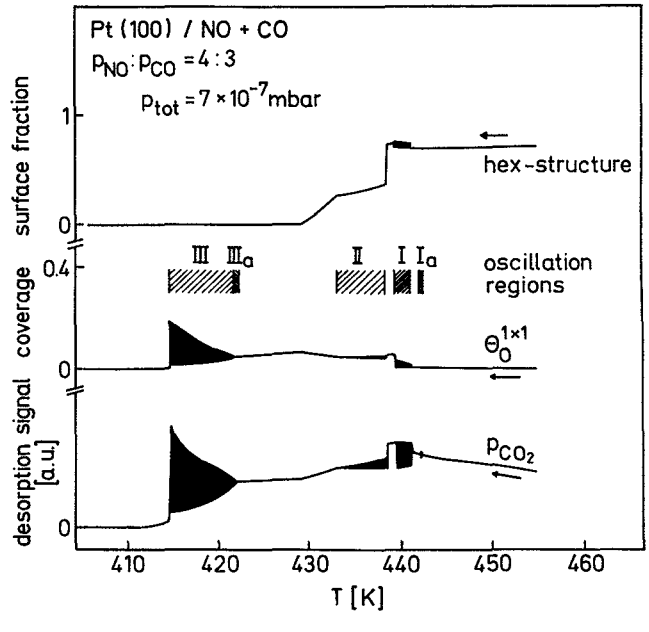

FIG. 11. Steady state values of CO_2 production, oxygen coverage ($\triangleq$ work function), and hex reconstructed surface on an enlarged section of the cooling branch of the hysteresis displayed in Fig. 10. Sustained oscillations with the amplitudes marked (black areas) occur in three regions (I, II, and III). In regions I(a) and III(a), damped oscillations are observed. Range I(a) also exhibits sustained oscillations, but with very low amplitude. While regions I and II can only be reached by moving along the cooling branch of the temperature hysteresis, range III exhibits oscillations independent of the initial conditions.

in region III proceed on a fully 1×1 surface. Since oscillations in regions I and II take place on a partially reconstructed surface, it is clear that these regions can only be reached when the system moves along the upper branch of the hysteresis from the fully hex structure, i.e., in the cooling direction. Oscillations in region III are always obtained in the calculations when temperature and pressure were chosen properly. They are independent of starting conditions which demonstrate that in region III there are no hysteresis phenomena.

The plot displayed in Fig. 11 represents a bifurcation diagram with the steady state values of the oscillation amplitudes outlined. Examples of sustained kinetic oscillations which exist in the regions I, II, and III are displayed in Fig. 12. Besides the regions of sustained oscillations, there exist parameter regions where the reaction approaches the stationary value of the reaction rate via damped oscillations. These regions are denoted by I(a) and III(a) in Fig. 11 and correspond to a stable focus in phase space located in the vicinity of the oscillatory regions.

As demonstrated by the example shown in Fig. 12(a), the simulated oscillations in region I are associated with periodic structural transformation via the $1\times1\rightleftharpoons$hex phase transition. Hence they obviously correspond to the experimental oscillations in the upper existence range in Fig. 1 (region I). As shown by the experimental results in Fig. 8, the oscillations proceed on a surface that is largely reconstructed, and which has a rather low adsorbate coverage. The same behavior is found with the simulated oscillations. The oscillation waveforms are quite different from sinusoidal in shape. They are more of the relaxation type.

The simulated oscillations in region III [Fig. 12(c)] evidently correspond to the experimental oscillations in the lower temperature experimental region (region II in Fig. 1). This conclusion follows from the fact that they proceed on a surface which remains entirely in a 1×1 state all the time. These oscillations are associated with relatively large variations in the adsorbate coverage. They also have correspondingly large amplitudes in rate oscillations. Thus the simulation reproduces both existence regions for kinetic oscillations. All essential features of the experimental findings, in particular, the role of the $1\times1\rightleftharpoons$hex phase transition, are also found in the results of the simulation.

In the simulation, however, an additional existence region (region II) for oscillations appeared which has no direct counterpart in the experiment. As demonstrated by the example displayed in Fig. 12(b), the oscillations in region II can be considered as an intermediate between the oscillations in region I and the oscillations in region III. They proceed on a partially reconstructed surface, but after an initial stepwise decrease, the hex area remains constant during the oscillations. Evidently the $1\times1\rightleftharpoons$hex phase transition is not involved in the steady state oscillations which take place on this partially reconstructed surface. Since the separation between regions I and II is quite small, it might well be that they were not recognized as two distinctly separate regions in the experiment. This conclusion appears quite realistic keeping in mind that only measurements of the reaction rate have been used in most cases in determining the existence regions for kinetic oscillations. Only in a few cases were

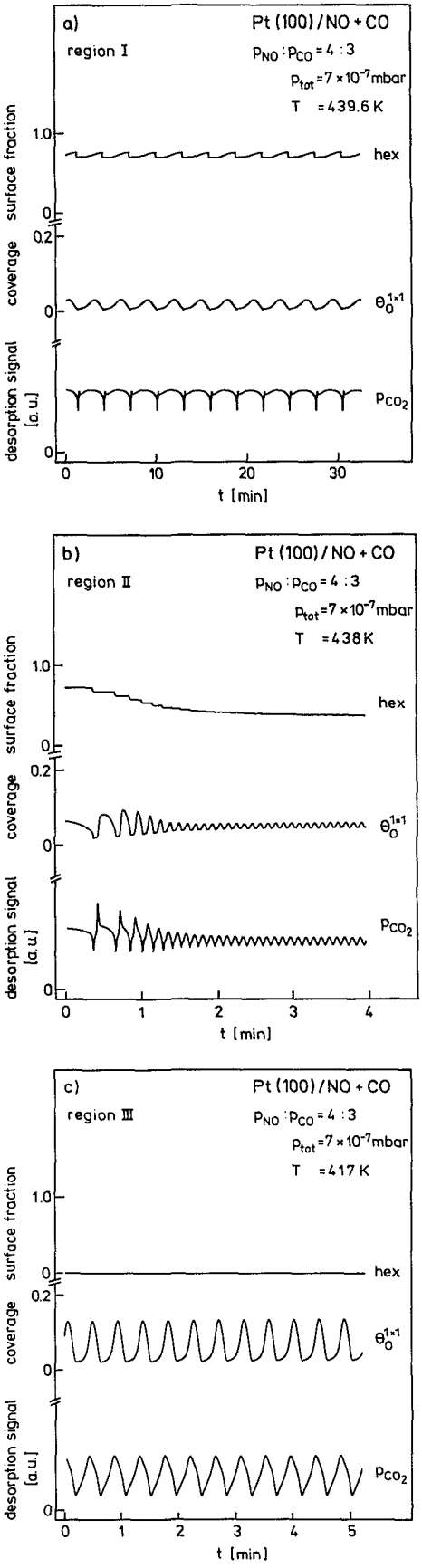

FIG. 12. Examples of oscillations in regions I, II, and III. The scaling of p_{CO_2}, θ_O, and the amount of the hex phase is always the same in order to make a comparison of amplitudes easier. (a) Region I [cf. Fig. 8(a)]; (b) Region II; (c) Region III [cf. Fig. 8(b)].

LEED measurements made in this regard.

If one compares the existence regions of the simulated and of the experimental oscillations, one realizes that they agree very well with respect to their absolute positions in temperature. Even the separating gap of ~15 K is identical to that of the experiment. Only the widths of the simulated and experimental regions still differ from each other. In Fig. 11, the temperature regions I and III are 3 and 8 K wide, respectively, while both existence regions in the experiment exhibit the same width of ~30 K. This discrepancy may at least be partially due to spatial inhomogeneities on the single crystal surface. According to the simulation results, these have a strong influence on kinetic oscillations and thus may cause a broadening of the existence regions.

The time scales of the simulated oscillations is the same as that of the experimental oscillations with periods likewise ranging from a few seconds to several minutes or even longer. Closer analysis of region III reveals a continuous increase of the oscillation period upon variation of the temperature from high to low values, where it tends toward infinity (Fig. 13). This behavior is in complete agreement with the experimental findings shown in Fig. 7 (except for the fact that the experimental oscillations were damped). This behavior is characteristic of a homoclinic bifurcation as mentioned before. Inspection of the bifurcation diagram of Fig. 11 indicates, on the other hand, that the onset of the oscillations at the high T boundary is associated with small amplitudes which continuously grow with decreasing temperature. Such a behavior is characteristic of a (supercritical) Hopf bifurcation.

The results of the simulation demonstrate that the kinetic oscillations in the Pt(100)/NO + CO system can be modeled qualitatively and even semiquantitatively exceedingly well. There exists, however, a fundamental difference with respect to the experimental results as the simulated oscillations are sustained, while the amplitude of the real oscillations decays in time. The origin of this discrepancy will be addressed in the next section.

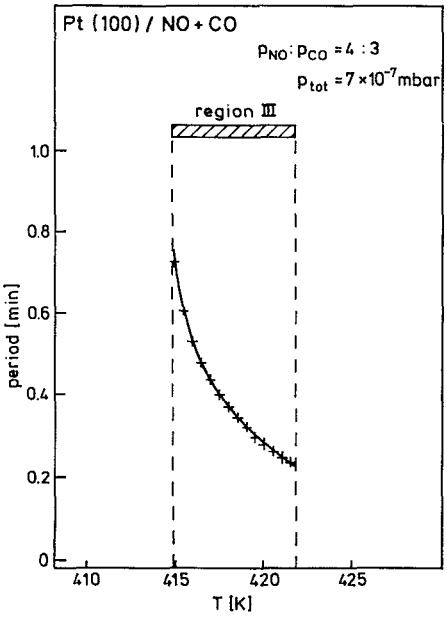

FIG. 13. Dependence of oscillation periods in region III on temperature to be compared with the experimental data for region II in Fig. 7.

C. Origin of the "damping" effect

Within the framework of nonlinear dynamics, damped oscillations correspond to a stable focus. Such foci usually exist in the vicinity of a Hopf bifurcation. Therefore it might well be that the accessible p_{CO}, p_{NO}, T-parameter range in our experiments corresponds to a region in the bifurcation diagram where a stable focus exists, while the Hopf bifurcation points are reached only at high pressures. Although such an explanation, in which the damping is due to the inherent dynamics of the oscillations, cannot be excluded, a different picture will be presented here. This is based on the following considerations:

In order to achieve measurable variations in the reaction rate, a synchronization mechanism for the local oscillators has to exist. Synchronization can be achieved via thermal coupling supplied by the reaction heat, via surface diffusion of a mobile adsorbate or via partial pressure changes in the gas phase that exist due to mass balance in the reaction.[35] Under the low pressure conditions of the single crystal studies here, only the latter two possibilities have to be taken into account. Temperature modulations are negligible. Gas phase coupling was found to be the dominant synchronization mode for the regular oscillations at high temperatures with the Pt(110)/CO + O_2 system.[35] The alternate case is represented by Pt(100)/CO + O_2, where the coupling between the surface reaction and CO surface diffusion causes the formation of propagating reaction fronts of macroscopic size.[11,12]

Scanning LEED experiments (albeit with a rather low spatial resolution of 0.5 mm) could not detect propagating reaction fronts with the present system. Thus, a synchronization mechanism via surface diffusion of CO or NO, analogous to that of the Pt(100)/CO + O_2 system, appears to be unlikely. A homogeneously oscillating surface could certainly be expected if gas phase coupling would provide an effective synchronization mode, but this mechanism requires the surface reaction to be sensitive to small variations in the gas phase concentrations. Such a mechanism can be excluded, as it was found with forcing experiments (the results of which are published separately)[20] that the modulation amplitude of p_{NO} and p_{CO} required for achieving entrainment greatly exceeded the amplitude of the p_{NO} and p_{CO} variations in the autonomously oscillating system.

Assuming the absence of an efficient synchronization mode, one can explain the damping effect in the following way: After the initial excitation by a small temperature step, all local oscillators start with the same phase. Due to inhomogeneities on the crystal surface, however, the initial spatial phase coherence is soon lost and the local oscillators will finally oscillate with a random phase relationship. This will lead to a decaying amplitude for the (integrated) rate oscillations until a stationary state is reached. This picture is supported by the experimental observation in Fig. 8(b) that the oscillations in the reaction rate, which is an integral over the whole surface area, decay much faster than the LEED inten-

sity oscillations. The LEED measurements sample only a small part of the surface area. This behavior is exactly what one would expect if a progressive loss in spatial coherence is responsible for the decreasing oscillation amplitude.

The transition from damped oscillations at low pressure to sustained oscillations at high pressure can be explained as being due to the development of an efficient synchronization mechanism via the nonisothermality of the reaction at high pressure. At high pressure ($p \sim 1$ atm), temperature oscillations of more than 20 K on supported Pt catalysts have been reported by Schüth and Wicke. This modulation of the sample temperature will cause a very strong thermal coupling of different parts of a catalyst.[10] In the experiments of Adlhoch and Lintz[8] at $\sim 10^{-4}$ mbar, the sample temperature was only measured as an integral value using the electrical resistance of their polycrystalline Pt foil sample. The large surface of this sample makes it possible that in these experiments, local temperature variations may also have occurred. An estimation of the maximum heat production for their sample resulted in a value of 900 mW. This is much more than the radiation loss and hence could have influence upon the sample temperature. During kinetic oscillations with periodic changes in heat production, our estimation leads to variations in the sample temperature of ~ 10 K amplitude.

The feasibility of such a thermal coupling mechanism can be further demonstrated by forcing experiments. A temperature modulation of more than 1 K amplitude proved to be sufficient to turn the damped oscillations on Pt(100) into sustained oscillations.[20] This gives additional support to the idea that the main difference between the simulated and the experimental oscillations produced at constant temperature is in fact the lack of an efficient spatial synchronization mode for the latter.

D. The simplified model

In both the experiment and in the simulation, it has been demonstrated that the $1 \times 1 \rightleftharpoons$hex phase transition is not crucial for the appearance of kinetic oscillations in the NO + CO reaction. It is therefore justifiable to simplify the system of DE's by freezing the surface in a 1×1 state. The above system of six DE's can thus be reduced to only three DE's.

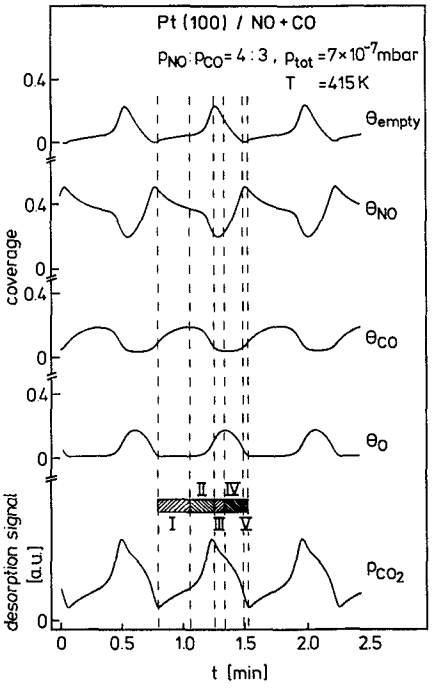

FIG. 14. Changes in the reaction rate and in the adsorbate composition during kinetic oscillations obtained with the simplified model of DE's. For a discussion of the mechanism, one oscillation period has been subdivided into five sections (see the text).

$$\frac{d\theta_{CO}}{dt} = k_1 p_{CO}(1 - \theta_{CO} - \theta_{NO}) - k_2\theta_{CO} - k_4\theta_{CO}\theta_O, \tag{I}$$

$$\frac{d\theta_{NO}}{dt} = k_1 p_{NO}(1 - \theta_{CO} - \theta_{NO}) - k_6\theta_{NO} - k_8\theta_{NO}\theta_{empty}, \tag{II}$$

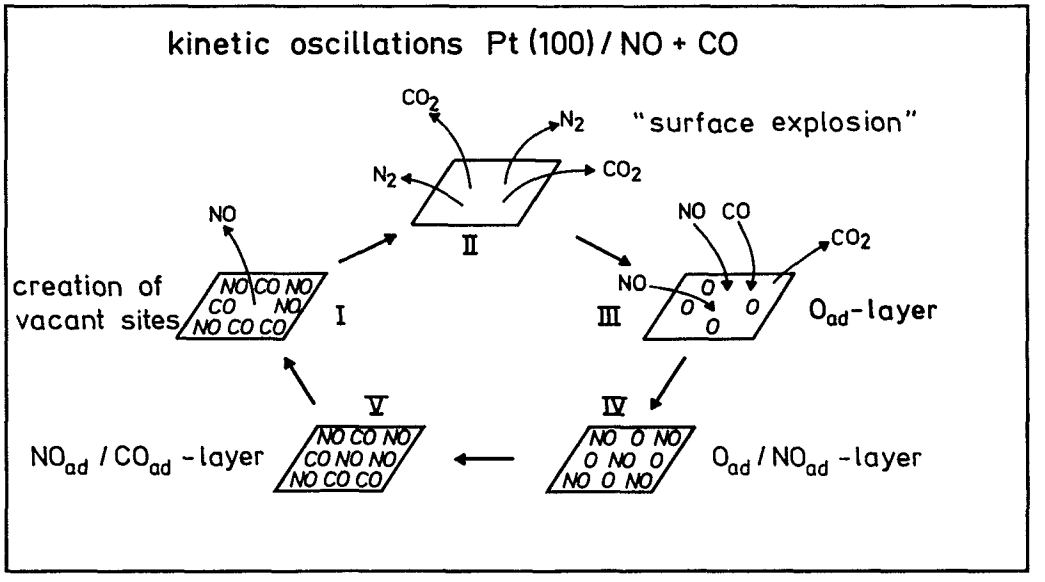

FIG. 15. A schematic diagram of the surface changes during one period of kinetic oscillations following the subdivision shown in Fig. 14.

$$\frac{d\theta_O}{dt} = k_8\theta_{NO}\theta_{empty} - k_4\theta_{CO}\theta_O, \qquad \text{(III)}$$

where

$$\theta_{empty} = \begin{cases} \left(1 - \dfrac{\theta_{NO}+\theta_{CO}}{\theta^{inh}_{CO,NO}} - \dfrac{\theta_O}{\theta^{inh}_O}\right), \\ \qquad \text{if } \left(1 - \dfrac{\theta_{NO}+\theta_{CO}}{\theta^{inh}_{CO,NO}} - \dfrac{\theta_O}{\theta^{inh}_O}\right) \geqslant 0 \\ 0, \qquad \text{otherwise.} \end{cases}$$

These equations utilize the same terms which were used in the realistic model to describe the adsorption/desorption of NO and CO on the 1×1 phase, the dissociation of NO and the surface reaction between O_{ad} and CO_{ad}. All terms involving the $1\times1 \rightleftharpoons$ hex phase transition have been dropped. The influence of surface defects is likewise neglected, since the 1×1 area already exhibits a high level of catalytic activity. The coverage dependence of the adsorption energies of CO and NO has been retained in the equations, since no oscillations could be obtained if these were held constant.

The numerical integration of the simplified system of DE's yields kinetic oscillations which are depicted in Fig. 14. These oscillations are the same as obtained with the full system of six DE's in region III. For a description of the mechanism, in Fig. 14 one oscillation cycle is subdivided into five sections. The individual stages in the mechanism which are displayed schematically in Fig. 15 can then be described as follows:

(I) *Creation of vacant sites.* We start with a mixed CO/NO adlayer, where the dissociation of NO and hence the surface reaction is inhibited due to a high adsorbate coverage. Initiated by CO/NO desorption, a few vacant sites are created so that NO can dissociate.

(II) *Autocatalytic reaction.* The increase in the number of vacant sites by the surface reaction [steps (R3), (R4), and (R5)] allows more NO to dissociate, thus starting the autocatalytic reactive removal of the molecular CO/NO adlayer. This step is identical to the so-called surface explosion in coadsorption experiments.[15,16]

(III) *Formation of an O adlayer.* The autocatalytic reaction creates an almost bare surface where adsorbed NO can dissociate without inhibition. The nitrogen which is formed desorbs immediately, but oxygen accumulates leading to the formation of an O adlayer. In this step, the gas phase ratio of $p_{NO}:p_{CO} > 1$ plays an important role.

(IV) *Replacement of O_{ad} by NO_{ad}.* With the oxygen coverage being high, the dissociation of NO becomes inhibited, but CO from the gas phase can still adsorb and react to form CO_2. The free adsorption sites which are thereby created by the reaction are preferentially populated by adsorbing NO. Thus the O adlayer is replaced by a NO adlayer.

(V) *Formation of a mixed NO/CO adlayer.* With decreasing oxygen coverage, the CO which adsorbs together with the NO is no longer removed by the surface reaction, but accumulates. This results in the buildup of a mixed NO/CO adlayer.

The mechanism described above explains kinetic oscillations in the Pt(100)/NO + CO system without the use of the $1\times1 \rightleftharpoons$ hex phase transition. The oscillations in the reaction rate are caused here by a periodic change of the surface between a state with low catalytic activity, where a high adsorbate coverage inhibits the dissociation of NO and a state with high catalytic activity, where a low coverage permits the dissociation of NO to take place.

There are two properties of the NO + CO system that keep it oscillating. First, the surface explosion (phase II) reduces the coverage within seconds by a factor of 2. At this

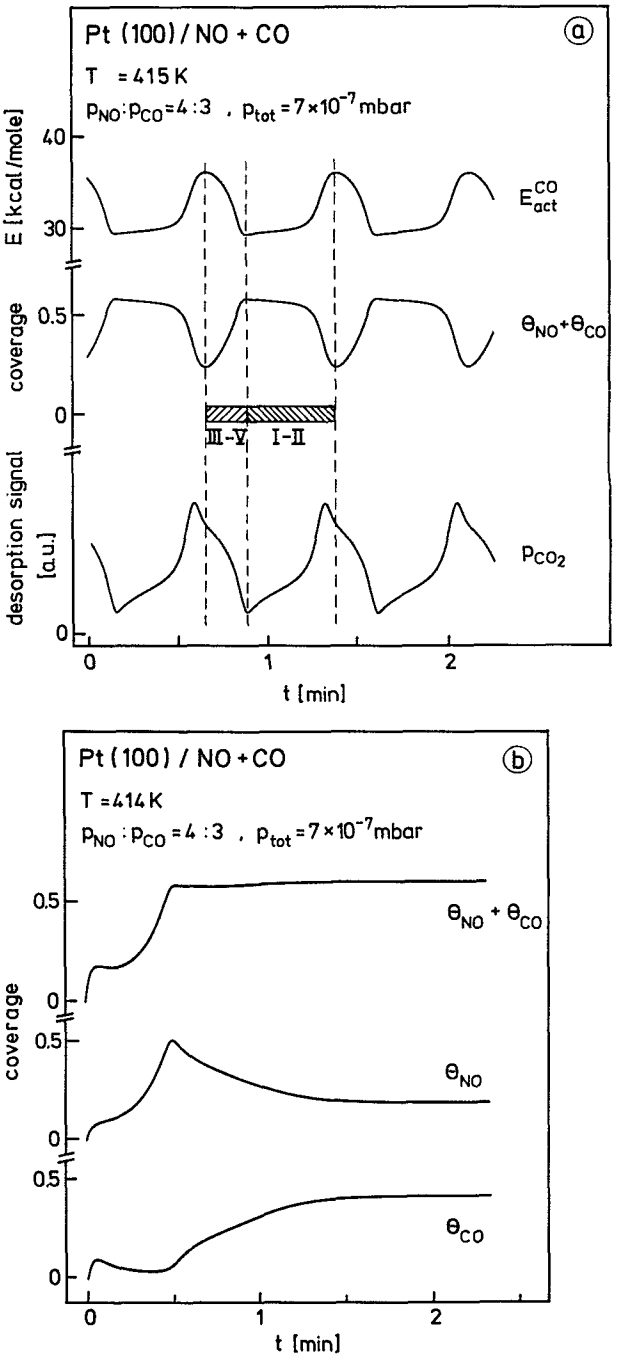

FIG. 16. (a) Changes in the reaction rate, the combined CO and NO coverage, and the adsorption energy of NO and CO during kinetic oscillations using the simplified system of DE's. (b) Establishing a stationary state at a temperature outside the oscillatory region. The starting point is an adsorbate-free 1×1 surface.

point, the coverage dependence of the adsorption energies of NO and CO which is displayed in Fig. 16(a) comes into play. Due to the drop in coverage, these energies increase in a short time and make adsorption favorable over desorption. After reestablishing a NO/CO adlayer, the cycle can start again. What is amazing at first sight is why the system does not reach a stationary state. This becomes clear by looking at the time scale of the oscillations and by comparing it to the time that is needed to reach a steady state at a somewhat lower temperature outside the oscillation region. As demonstrated by Fig. 16(b), the time which is required to reach a steady state under these conditions is considerably larger than one oscillation period. Without coverage-dependent adsorption energies, however, steady state coverages are reached so fast that no oscillations occur.

In order to explain the mechanism of kinetic oscillations which involve the $1\times1\rightleftharpoons$hex phase transition (region I), no new principles have to be introduced. In addition to the mechanistic steps discussed above, one just has to consider the relaxation of the surface structure according to the variation of the adsorbate coverages. Starting with dense 1×1-NO/CO islands, the onset of the autocatalytic reaction will create adsorbate-free 1×1 areas which relax back into the hex structure. As soon as the oxygen coverage on the remaining 1×1 area drops to a low enough level, CO is no longer consumed by the reaction, but its coverage increases due to trapped CO molecules from the surrounding hex area. The increase in CO coverage causes the 1×1 islands to grow, thus reversing the $1\times1\rightarrow$hex phase transition that took place in the preceding step. Simultaneously, with the growth of 1×1 islands, coadsorption of NO will take place leading to the formation of mixed 1×1 NO/CO islands and the initial situation is reached again.

V. DISCUSSION

The replacement of O_2 by NO as oxidizing agent in the reaction of CO on Pt(100) leads to the occurrence of some new phenomena: surface explosion in coadsorption experiments and damped kinetic oscillations under continuous flow conditions. The latter do not necessarily require the participation of the $1\times1\rightleftharpoons$hex phase transition as is the case with CO + O_2. Moreover, the phenomenology of the oscillations is quite different in both systems. The oscillations with NO + CO are always very regular and well reproducible, while the oscillations in the CO + O_2 reaction are mostly irregular and difficult to reproduce. These differences between the two reaction systems are a consequence of the different degree of spatial organization. While the oscillations in the NO + CO reaction appear to proceed spatially homogeneously on a macroscopic scale, the CO + O_2 reaction exhibits a quite different behavior: Spatial inhomogeneities and propagating chemical waves on a macroscopic scale have been detected.[12,36]

The reason for these differences lies obviously in the different adsorption properties of NO and O_2. In the case of oxygen, the adsorption probability on Pt(100) depends strongly on the surface structure. The two phases hex and 1×1 differ in the oxygen sticking coefficient by a factor of ~1000. The hex phase is quite inactive for oxygen adsorption. The active 1×1 phase, however, must first be prepared by the CO-induced hex$\rightarrow1\times1$ phase transition. In effect, this leads to the development of spatial inhomogeneities, since separate islands of CO and oxygen will be formed as a consequence of the different adsorption properties of the two surface phases. The surface reaction now has to proceed at the boundaries of the islands. This explains the occurrence of propagating reaction fronts in a hole-eating mechanism.[11,36] By way of contrast, in most adsorption properties NO behaves very similarly to CO.[16] As a consequence, both adsorbates form mixed NO + CO islands[13,16] and therefore the reaction is not limited to the boundaries of the islands, but may well proceed inside. In this way, one can understand that no reaction fronts of macroscopic size develop in the NO + CO reaction on Pt(100). The question how the spatial self-organization proceeds on a mesoscopic and microscopic length scale still needs to be answered by experiment with a spatially resolving technique. Such experiments which are planned for the future are also necessary in order to decide whether the damping effect is in fact caused by a progressive loss of spatial coherence in the oscillations, or whether it is due to the dynamical properties of a local oscillator.

As was shown in Sec. IV D, the autocatalysis in the surface reaction in combination with the coverage dependence of the desorption parameters for NO and CO is sufficient to produce kinetic oscillations; an involvement of periodic structural changes is not essential for the oscillating mechanism. It is then of course not clear why kinetic oscillations in the NO + CO reaction were only observed on Pt(100), but not with other low-index orientations which have been investigated as well, but the relevant surface property for the surface explosion as well as for the kinetic oscillations has been shown to be the dissociation efficiency of NO. This quantity depends sensitively on the surface structure. It is rather high for Pt(100) with a dissociation probability of $\sim60\%$, but roughly one order of magnitude lower on Pt(110) with $\sim10\%$ and very low for Pt(111), where it is in the order of a few percent.[37,38] Thus the autocatalysis mechanism outlined in Sec. IV D is suppressed for these orientations and no kinetic oscillations can be expected.

For most of the high-index Pt surfaces, the NO dissociation probability is comparable to the (100) plane. The most active plane with respect to NO decomposition is the (410) orientation with $\sim100\%$ dissociation efficiency.[37,38] On this plane also, a surface explosion in NO + CO coadsorption experiments was observed.[26] Therefore Pt(410) might be a good candidate for exhibiting kinetic oscillations.

Polycrystalline Pt is known to exhibit both surface explosion and kinetic oscillations.[8,39] In this case, most probably (100) orientations in the texture of the polycrystalline materials are responsible for both phenomena, while the predominant (111) orientations should be inactive. In experiments at high pressure, when the 1×1 structure is permanently stabilized by adsorbates and unavoidable impurities, the $1\times1\rightleftharpoons$hex phase transition will no longer proceed. Since the simplified system of DE's does not require the presence of a phase transition, however, our model should be equally applicable to kinetic oscillations on polycrystalline Pt.

VI. CONCLUSIONS

Steady states and the appearance of kinetic oscillations in the catalytic NO + CO reaction on Pt(100) were investigated under continuous flow conditions in the 10^{-6} mbar range. Two stable branches of the reaction have been identified. These are related to different structural composition of the surface. On one of these branches, kinetic oscillations were found in two temperature regions of about 30 K width. These regions were separated by a gap of ~ 15 K. The oscillations were observed to be always damped. They could be excited by slightly decreasing the temperature. In the high-temperature region, video-LEED measurements revealed periodic changes in surface structure with low amplitude, while in the low-temperature region of oscillations, the oscillations take place on a surface that is completely in the 1×1 structure. These results stimulated the search for a model that could explain the oscillations without involvement of a periodic $1\times1\rightleftharpoons$hex phase transition. A set of coupled differential equations describing the elementary steps of the reaction was able to model nearly all properties of the NO + CO reaction excellently. Besides explaining the so-called surface explosion on which we reported in an earlier paper,[15] the model calculations yielded the steady states of the reaction as well as the occurrence of kinetic oscillations in three different regions. Two of these regions were in complete agreement with experimental evidence, whereas the third region has not been identified in experiment. In the case that oscillations take place on a pure 1×1 surface, the model reduces to only three DE's. In this simplified model, the oscillation mechanism can be seen as a periodic sequence of autocatalytical surface explosions and restorations of the initial adsorbate coverage. The damping of the oscillations in our experiments is attributed to insufficient thermal coupling caused by the small exothermicity of the reaction at low pressure. The existence of sustained oscillations on polycrystalline Pt on the other hand can be traced back to the nonisothermality of the reaction at high pressure ($p > 10^{-4}$ mbar).

ACKNOWLEDGMENTS

Financial support by the Alexander von Humboldt Foundation (J.-P. D.) is gratefully acknowledged. We also would like to thank S. Wasle for technical assistance and the preparation of the drawings. The authors are also indebted to H. H. Madden for carefully reading the manuscript.

[1] P. Hugo, Ber. Bunsenges Phys. Chem. **74**, 121 (1970).
[2] H. Beusch, P. Fieguth, and E. Wicke, Chem. Ing. Tech. **44**, 445 (1972).
[3] R. Imbihl, in *Springer Series in Synergetics*, edited by P. J. Plath (Springer, Berlin, 1989), Vol. 44, pp. 26-64.
[4] G. Ertl, Adv. Catal. **37**, 213 (1990).
[5] S. P. Singh-Boparai and D. A. King, in: Proceedings of the 3rd European Conference on Surface Science (ECOSS-3), Cannes, 1980.
[6] S. B. Schwartz and L. D. Schmidt, Surf. Sci. **183**, L269 (1987).
[7] S. B. Schwartz and L. D. Schmidt, Surf. Sci. **206**, 169 (1988).
[8] W. Adlhoch, H.-G. Lintz, and T. Weisker, Surf. Sci. **103**, 576 (1981).
[9] H. Bolten, T. Hahn, J. Le Roux, and H. G. Lintz, Surf. Sci. **160**, L529 (1985).
[10] F. Schüth and E. Wicke, Ber. Bunsenges Phys. Chem. **93**, 191 (1989); **93**, 491 (1989).
[11] R. Imbihl, M. P. Cox, G. Ertl, H. Müller, and W. Brenig, J. Chem. Phys. **83**, 1578 (1985).
[12] R. Imbihl, M. P. Cox, and G. Ertl, J. Chem. Phys. **84**, 3519 (1986).
[13] W. F. Banholzer and R. I. Masel, Surf. Sci. **137**, 339 (1984).
[14] M. W. Lesley and L. D. Schmidt, Surf. Sci. **155**, 215 (1985).
[15] Th. Fink, J.-P. Dath, M. R. Bassett, R. Imbihl, and G. Ertl, Vacuum **41**, 301 (1990).
[16] Th. Fink, J.-P. Dath, M. R. Bassett, R. Imbihl, and G. Ertl, Surf. Sci. **245**, 96 (1991).
[17] K. Besocke and S. Berger, Rev. Sci. Instrum. **47**, 840 (1976).
[18] R. J. Behm, P. A. Thiel, P. R. Norton, and G. Ertl, J. Chem. Phys. **78**, 7437 (1983); **78**, 7448 (1983).
[19] M. Eiswirth, R. Schwankner, and G. Ertl, Z. Phys. Chem. N. F. **144**, 59 (1985).
[20] J.-P. Dath, Th. Fink, R. Imbihl, and G. Ertl, J. Chem. Phys. (submitted).
[21] H. P. Bonzel, G. Brodén, and G. Pirug, J. Catal. **53**, 96 (1978).
[22] J. L. Gland, Surf. Sci. **71**, 327 (1978).
[23] R. L. Klein, S. Schwartz, and L. D. Schmidt, J. Phys. Chem. **89**, 4908 (1985).
[24] W. Adlhoch and H.-G. Lintz, Surf. Sci. **78**, 58 (1978).
[25] A. E. Morgan and G. A. Somorjai, Surf. Sci. **12**, 405 (1968).
[26] Y. O. Park, W. F. Banholzer, and R. I. Masel, Surf. Sci. **155**, 341 (1985).
[27] K. Heinz, E. Lang, K. Strauss, and K. Müller, Appl. Surf. Sci. **11/12**, 611 (1982).
[28] P. R. Norton, J. A. Davies, D. K. Creber, C. W. Sitter, and T. E. Jackman, Surf. Sci. **108**, 205 (1981).
[29] K. Griffiths, T. E. Jackman, J. A. Davies, and P. R. Norton, Surf. Sci. **138**, 113 (1984).
[30] P. Gardner, M. Tüshaus, R. Martin, and A. M. Bradshaw, Surf. Sci. **240**, 112 (1990).
[31] R. J. Gorte, L. D. Schmidt, and J. L. Gland, Surf. Sci. **109**, 367 (1981).
[32] C. T. Campbell, G. Ertl, H. Kuipers, and J. Segner, J. Chem. Phys. **73**, 5862 (1980).
[33] G. Pirug and H. P. Bonzel, J. Catal. **50**, 64 (1977).
[34] R. J. Gorte and L. D. Schmidt, Surf. Sci. **111**, 260 (1981).
[35] M. Eiswirth, P. Möller, K. Wetzl, R. Imbihl, and G. Ertl, J. Chem. Phys. **90**, 510 (1989).
[36] Th. Fink, R. Imbihl, and G. Ertl, J. Chem. Phys. **91**, 5002 (1989).
[37] W. F. Banholzer, Y. O. Park, K. M. Mak, and R. I. Masel, Surf. Sci. **128**, 176 (1983).
[38] Y. O. Park, W. F. Banholzer, and R. I. Masel, Appl. Surf. Sci. **19**, 145 (1984).
[39] H. Miki, T. Nagase, T. Kioka, S. Sugai, and K. Kawasaki, Surf. Sci. **225**, 1 (1990).